

**Comprehensive Single and Paired Drug Target
Identification in Healthy and Disease Models of NF-kB
Pathway**

by

Sahar Ashraf Alkhairy

Submitted to the Department of Electrical Engineering and Computer
Science

in partial fulfillment of the requirements for the degree of

Masters of Engineering in Computer Science and Molecular Biology

at the

MASSACHUSETTS INSTITUTE OF TECHNOLOGY

June 2016

© Massachusetts Institute of Technology 2016. All rights reserved.

Author
Department of Electrical Engineering and Computer Science
March 22, 2016

Certified by
Bruce Tidor
Professor of Biological Engineering and Computer Science
Thesis Supervisor

Accepted by
Christopher J. Terman
Department Committee on Graduate Theses

Comprehensive Single and Paired Drug Target Identification in Healthy and Disease Models of NF- κ B Pathway

by

Sahar Ashraf Alkhairy

Submitted to the Department of Electrical Engineering and Computer Science
on March 22, 2016, in partial fulfillment of the requirements for the degree of
Masters of Engineering in Computer Science and Molecular Biology

Abstract

Nuclear NF- κ B ("NF- κ Bn") is a transcription factor responsible for regulating many genes that play important roles in inter- and intra-cellular signaling, cellular stress responses, cell growth, survival and apoptosis. Defective levels of NF- κ Bn has been associated with cancer, inflammatory, and autoimmune diseases. Therefore, it is important to identify species in the NF- κ B pathway that if inhibited/ targeted by added drugs normalize the levels of NF- κ Bn. Also, since there is a limit to how effective single drug targets are in complicated diseases, identification of combinations of targets is very important. Existing experimental and computational work are disease specific, not comprehensive as they only analyze specific drug targets, and rarely analyze combinations of targets. In this thesis, we computationally modify a healthy model of the pathway to reflect what is defective in different classes of diseases. Then for each of the healthy and disease models, we score individual targets based on how much change in concentration of NF- κ Bn they induce when inhibited with an added inhibitor. Furthermore, we explain (1) why certain species score better than others, (2) why the inhibition profile of the output (NF- κ Bn) is not linear, and (3) why some isoforms of the same species score better than others. We also classify pairs of targets based on whether they are synergistic, additive, or antagonistic and obtain general trends for synergism of target combinations. Finally, we provide a comparison of the identified best targets with previously identified ones. One of our main findings is that very few species are effective at low levels of inhibition but many are effective at extremely high levels of inhibition. We also find that the scores of the species greatly depend on their steady state concentrations, the relative reaction parameters such as nuclear import/export rates and synthesis rates, and the relative concentrations of IKK and NF- κ B. Furthermore, we find that all species that have some effect on the output are synergistic with one another. In departure from other approaches we have computationally targeted both individual proteins and protein complexes, rather than just individual proteins. Although protein complexes score better they are more difficult to inhibit physically.

Thesis Supervisor: Bruce Tidor

Title: Professor of Biological Engineering and Computer Science

Acknowledgments

I would like to thank my direct supervisor David Flowers for his invaluable supervision, Nirmala Paudel for her great help as this thesis is based on her PhD thesis work, the rest of the Tidor lab for producing a great work environment, Prof. Bruce Tidor for his supervision, and my parents and siblings for their eternal love and support.

Contents

1	Introduction	11
1.1	Background and Motivation	11
1.2	Previous Work	12
1.3	Objectives	13
1.4	Organization	13
2	Models	15
2.1	Healthy Model	15
2.1.1	The System	15
2.1.2	System's Behavior	16
2.2	Diseases Associated with Defective NF- κ B Output	17
2.2.1	Associated Diseases	17
2.2.2	Disease Model 1: Loss of I κ Bs Function	18
2.2.3	Disease Model 2: Inactive IKK	18
2.2.4	Disease Model 3: Constitutively Active IKK	18
3	Methodology	21
3.1	Targeting and Scoring of Individual Species	21
3.2	Targeting Pairs of Species and Categorizing Them	22
3.3	Features	23
4	Model Results	25
4.1	Disease Model 1: Loss of I κ Bs Function	25

4.2	Disease Model 2: Inactive IKK	26
4.3	Disease Model 3: Constitutively Active IKK	26
4.4	Disease Models Used in Identifying Targets	27
5	Single Target Results	29
5.1	Single Drug Targets in the Healthy Model	29
5.1.1	Output Effect - Inhibition Level Profiles for Each Target	29
5.1.2	Optimal Target and TE level	30
5.1.3	Optimal Target	32
5.1.4	TE Level Threshold	32
5.2	Single Drug Targets in Disease Model 1	32
5.2.1	Output Effect - Inhibition Level Profiles for Each Target	32
5.2.2	Optimal Target and TE level	33
5.2.3	Optimal Target	35
5.2.4	TE level Threshold	35
5.3	Single Drug Targets in Disease Model 3	35
5.3.1	Output Effect - Inhibition Level profiles for each Target	35
5.3.2	Optimal Target and TE level	36
5.3.3	Optimal Target	38
5.3.4	TE Level Threshold	38
5.4	Comparison of Single drug targets across models	38
6	Paired Target Synergy Results	41
6.1	Paired Drug Targets in the Healthy Model	41
6.2	Paired Drug Targets in Disease Model 1	42
6.3	Paired Drug Targets in Disease Model 3	43
6.4	Paired Drug Targets Across Models	44
7	Discussion	45
7.1	Explanation of Top Scoring Single Targets	45
7.2	Why does the output, NF- κ Bn, not have a linear profile?	52

7.3	Why are alpha isoforms better drug targets than the beta and epsilon isoforms?	53
7.4	Combination of Targets Classification	58
7.5	Comparison of Identified Drug Targets to Existing Ones	60
8	Conclusion	63
A	Tables	65
A.1	Healthy NF- κ B Model Species and Their Initial Concentrations.	65
A.2	Healthy NF- κ B model reactions and their rates	67
B	Figures	71
B.1	NF- κ B Model	71
B.2	OE vs TE Species Profiles for the Healthy Model	72
B.3	OE vs TE Species Profiles for Disease Model 1	74
B.4	OE vs TE Species Profiles for Disease Model 3	76
B.5	Synergism Classifications	78

Chapter 1

Introduction

1.1 Background and Motivation

Nuclear NF- κ B (NF- κ Bn) is a transcription factor that is responsible for regulating many genes that play important roles in inter- and intra-cellular signaling, cellular stress responses, cell growth, survival and apoptosis [1]. Studies have found that many diseases are associated with a defective level of NF- κ Bn such as chronic inflammatory and autoimmune diseases (eg. asthma, COPD, and Celiac disease) [2,3].

Inhibiting the NF- κ B pathway by inhibiting its species (proteins/ protein complexes) would normalize the output of NF- κ Bn. However, inhibition of the various species in the pathway do not all have the same level of effect on NF- κ Bn's output level. A few species might greatly increase/ decrease NF- κ Bn's output when inhibited by an added drug (inhibitor), while other species might have negligible effects. Therefore, identification of the best individual species (drug targets) to target is very important.

Furthermore, in many complex diseases like cancer there is a limit to how effective a single drug target is in normalizing the output either because of drug resistance or due to narrow therapeutic windows. Combination therapy, in which two or more drug targets are inhibited simultaneously, has emerged as a potential way to circumvent some of these shortcomings. The drug combinations may be additive, synergistic, or antagonistic. An additive pair is one in which a linear combination of the two drug concentrations leads to the same overall effect on the output. A synergistic pair is one in which the addition

of one of the drugs reduces the amount required of the second drug to obtain an equal overall output effect compared to a linear combination of the two, requiring an overall lower amount of total drug intake. An antagonistic pair is one where we need a greater total amount of drug to have the same effect on the output than if only one of the drugs was given. Therefore, classification of target combinations in terms of synergism is another very important objective as we would like to simultaneously target species that are synergistic with one another and not antagonistic.

Screening drug targets in labs is expensive and time-consuming, thus comprehensively screening all the species in the pathway is extremely costly and technically infeasible. Computational comprehensive identification of drug targets, using computational models of the pathway, is faster, less expensive and provides a holistic view of the pathway. Thus this thesis takes a computational approach.

1.2 Previous Work

There have been great work towards the goal of identifying drug targets in the NF- κ B pathway. Experimental work by Luron et al. [4], Trepicchio et al. [5], and Gohda et al. [6] focus on identifying drugs(s) for only a specific target and/ or analyzing if an existing drug that treats another disease would treat a disease associated with NF- κ B pathway and then identifying the point of inhibition. Other more comprehensive experimental work like Miller et al.'s [7], start with many clinically approved drugs and screen them to identify the ones that inhibit the NF- κ B signalling and then identify the points of inhibition.

As computational modeling can provide strong quantitative predictions, there have been computational work that also have the goal of identifying drug targets in the NF- κ B pathway. Zhou et al. [8] analyzed the inhibition effects of four existing drugs and their targets individually and in combinations using a NF- κ B pathway model with parameters obtained from cells with multiple myeloma.

These excellent works use cell lines or models that are disease specific. They are also not comprehensive and are limited to the analyses of previously identified drugs and their targets missing out on other potentially good targets. While there have been comprehensive

analyses of the NF- κ B pathway such as the work of Kell et al. [9], they usually have the goal of analysing cellular signalling interactions by identifying the parameters that have the most control on the oscillatory output of NF- κ Bn which is different than the goal of identifying drug targets.

1.3 Objectives

There are five main objectives to this thesis. The first is to identify the points of defects in the pathway that are the cause for disease and modify the healthy model to reflect that in order to allow for a more robust way of discovering drug targets for different diseases. The second is to obtain the best individual drug targets in the healthy and disease models. The third is to categorize the target combinations as additive, synergistic, or antagonistic. The fourth is to provide explanations to why certain targets score better than others and explanations to key observations. The two key observations are (1) Why does the output, NF- κ Bn, not have a linear profile? (2) Why are alpha isoforms better drug targets than the beta and epsilon isoforms? The fifth is to provide a comparison of the identified best targets with previously identified ones.

1.4 Organization

This thesis consists of six main chapters. In Chapter 2, we describe the healthy and disease models of NF- κ B. In Chapter 3, we describe the methodology used for scoring individual species and the categorization of combinations of species. In Chapter 4, we show how the output changes with the different disease models and determine if the objective is to increase or decrease the output. In Chapter 5, we present the scoring results of the individual species for the different models. In Chapter 6, we present the categorization results of the combinations of species. In Chapter 7, we provide explanations to the results obtained and compare the identified targets to previously identified ones.

Chapter 2

Models

2.1 Healthy Model

2.1.1 The System

The deterministic NF- κ B pathway model by Kell et al [9] is periodic and contains species in both the nucleus and the cytoplasm. It contains 26 species (including the source which represents DNA and the sink which represents degradation) (table A.1 in Appendix A) and 64 mass actions reactions modeled by ordinary differential equations (table A.2 in Appendix A). There are 3 negative regulators for NF- κ B: $I\kappa B\alpha$, $I\kappa B\beta$, and $I\kappa B\epsilon$; and one kinase (IKK) that phosphorylates the inhibitors for degradation. All the $I\kappa$ Bs are similar in structure but have different binding preferences. In general, NF- κ B can either be p65/p50 or p50/p50. The p65/p50 leads to the transcription of a variety of genes, and the p50/p50 homodimer inhibits transcription [10]. The NF- κ B that is in the model is the p65/p50 [9].

There are approximately seven surface receptors that are upstream of the NF- κ B pathway and they are: BCR, TCR, TLRs, IL-1R, TNFR, GF-Rs, and (LTBR, CD40, BR3) [11]. In the model used, the pathway is activated by TNF-a. The activation of TNF-a leads to activation of IKK, which in turn phosphorylates the inhibitor-NF- κ B complex ($I\kappa$ B-NF- κ B), which leads to ubiquitination of the inhibitors and release of NF- κ B, which then enters the nucleus and transcribes proteins including its inhibitors.

The model includes only the core of the NF- κ B pathway and does not include the

surface receptors mentioned above. However, the stimulation of IKK by the TNF- α surface receptor and other means is captured by having the concentration of IKK to be initially at $0.1 \mu M$ and then having it gradually decrease (as the stimulation goes away). A very simplified version of the pathway is shown in figure 2-1. A more detailed pathway is found in figure B-1 in Appendix B.

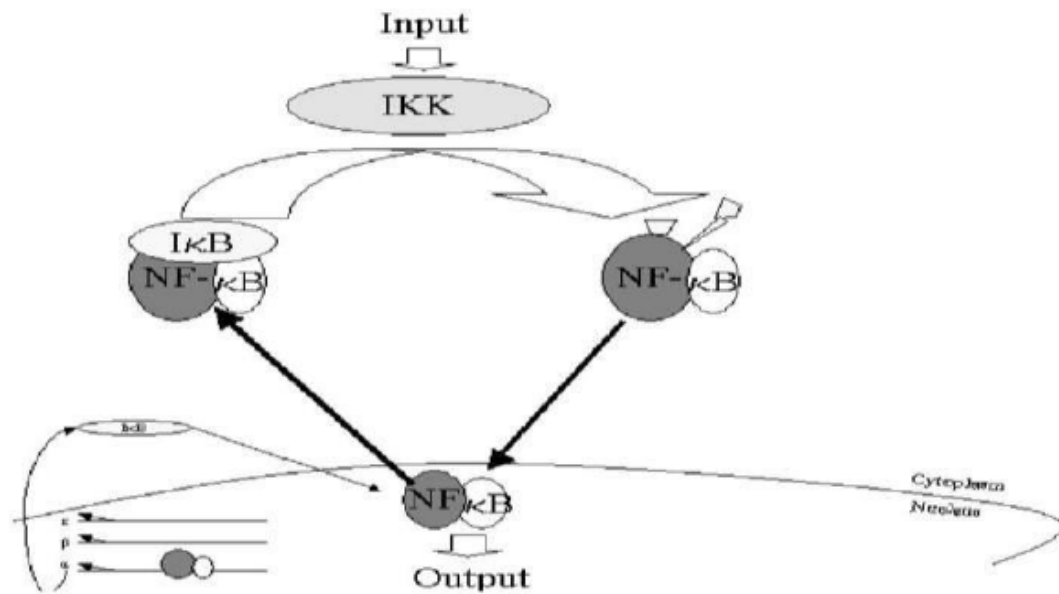


Figure 2-1: A simplistic overview of the NF- κ B pathway. Source Kell et al. [9]

2.1.2 System's Behavior

The System at the Beginning and After Reaching Steady State

The system starts off with $I\kappa B_x$, $I\kappa B_{xn}$, $NF-\kappa B$, $NF-\kappa B_n$, $I\kappa B_x-NF-\kappa B$, $I\kappa B_{xn}-NF-\kappa B_n$, IKK , and $I\kappa B_x-t$ where x refers to all three isophorms alpha, beta, and epsilon. All complexes with IKK start off with zero concentration. The species that get degraded are IKK , $I\kappa B_x$, $I\kappa B_x-t$. $I\kappa B_x-t$ gets produced continuously, $I\kappa B_{\alpha-t}$ at a rate of $1.54 * 10^{-6} \mu M^{-1} s^{-1}$, $I\kappa B_{\beta-t}$ at a rate of $1.78 * 10^{-7} \mu M^{-1} s^{-1}$, and $I\kappa B_{\epsilon-t}$ at a rate of $1.27 * 10^{-7} \mu M^{-1} s^{-1}$.

After running the system to steady state, most of the species have a steady state concentration approximately the same as the starting concentrations except IKK which gets completely degraded. Complexes with NF- κ B and NF- κ Bn have a steady state concentration slightly higher than the initial starting concentration. The output of concern, NF- κ Bn, reaches steady state after many oscillations. The area under the curve is 24.1600 μ M with peak amplitude of 0.0002 μ M and steady state concentration of $2.4 * 10^{-4} \mu$ M.

2.2 Diseases Associated with Defective NF- κ B Output

2.2.1 Associated Diseases

IKK is composed of 3 subunits: IKK1(IKK α), IKK2(IKK β), and NEMO(IKK γ). IKK1 and IKK2 are catalytic subunits, whereas NEMO is a regulatory subunit. When ligands bind to the surface receptors, after a cascade of signals, NEMO either get activated or inhibited by different upstream species [10].

Diseases associated with NF- κ B are caused by alterations to 'healthy' resulting from defects in (1) NF- κ B itself, (2) species that directly regulate NF- κ B but are not in our model, (3) I κ Bs, (4) IKK (especially NEMO), or (5) species upstream of IKK [12]. We only consider diseases caused by the last three types (3, 4, 5) of modification.

An example of a disease caused by modifications in I κ Bs is HL (common B-cell lymphoma). In this disease, the I κ Bs lose their function thereby leading to a constitutively active NF- κ B [12].

Our model does not include species upstream of IKK and furthermore treats IKK1 (IKK α), IKK2 (IKK β), and NEMO (IKK γ) as one species - IKK. Thus we can collapse the alterations (4) and (5) into ones with inactive IKK and ones with a constitutively active IKK. The first category (ones with inactive IKK) causes a decrease in NF- κ B activation and the second category (ones with constitutively active IKK) causes an increase in NF- κ B activation.

Examples of diseases that belong to the first category are incontinentia pigmenti (IP) [13], a genetic disease that causes altered pigmentation and developmental abnormalities,

and anhidrotic ectodermal dysplasia with immunodeficiency (EDA-ID) [12], a group of conditions characterized by abnormal development of ectodermal tissues including the skin, hair, teeth, and sweat glands. An example of a disease that belongs to the second category is Multiple Myeloma, cancer that forms in plasma cells [14]. It is important to note that there are extremely rare diseases that are caused by $I\kappa B\alpha$ not getting phosphorylated by IKK such as EDA-ID(t), but they are not considered as they are very rare [12].

To summarize, the three disease models we will study are: (1) Model 1: Loss of $I\kappa B$ s function, (2) Model 2: inactive IKK, (3) Model 3: constitutively active IKK.

2.2.2 Disease Model 1: Loss of $I\kappa B$ s Function

HL (common B-cell lymphoma) is disease caused by modifications in $I\kappa B$ s such that they lose their functionality. In the original healthy model, we start off with initial amounts of $I\kappa B$ s that gets degraded and consumed by reactions but gets replenished at a constant rate. In order to alter the model to have it represent the disease state with dysfunctional $I\kappa B$ s, we change the concentrations of the three $I\kappa B$ s to be constant at zero. This is to show that even though $I\kappa B$ s are being produced, only dysfunctional ones are. Changing the concentration of transcriptional $I\kappa B$ s to be constant at zero produces the exact same results as when we modified the concentrations of $I\kappa B$ s. We will use the model in which the concentrations of the three transcriptional $I\kappa B$ s are set constant at zero.

2.2.3 Disease Model 2: Inactive IKK

Incontinentia pigmenti (IP) is a disease caused by an inactive IKK component NEMO. In the healthy model we have an initial amount of $0.1 \mu\text{M}$ of IKK which is consumed and degraded over time. In order to alter the model to have it represent the disease state with an inactive IKK, we make IKK be a constant input at $0 \mu\text{M}$.

2.2.4 Disease Model 3: Constitutively Active IKK

Multiple Myeloma is a disease caused by having a constitutively active IKK. The initial amount of IKK ($0.1 \mu\text{M}$) gets consumed and degraded over time. In order to alter the model

to have it represent the disease state with a constitutively active IKK, we make IKK be a constant input at $0.1 \mu\text{M}$.

Chapter 3

Methodology

Our methods are based on Nirmala's methodology [15] to target individual and pairs of species, score individual species, and categorize pairs of targets.

3.1 Targeting and Scoring of Individual Species

One of our main objectives is to exhaustively identify the best individual drug targets that either decrease the output in diseases that have an increased output or increase it in diseases that have a decreased output. In order to achieve that objective and identify the best individual targets, we systematically add a constant amount of reversible inhibitor to each species with an association rate constant of $10^{-3}\mu M^{-1}s^{-1}$ and a dissociation rate constant of $10^{-6}s^{-1}$ (inhibitor constant of $10^{-3}\mu M$) at 100 different logarithmically spaced concentrations between 10^{-4} and $10^2\mu M$. We maintain the inhibitor at a constant value to simulate having a large amount of drug in the system.

To quantify the effect of the inhibition on the output we obtain the target effect (TE) and output effect (OE) for each of the 100 different inhibitor concentrations after allowing the system to equilibrate with the inhibitor and reach steady state to get rid of transient fluctuations that are a result of initial concentrations. The target effect is the fraction of available target that is bound by inhibitors, which is inactive and cannot participate in reactions. The output effect is the percentage change in output from the unperturbed state; It is the percent decrease in diseases with a higher than normal output and a percent increase

in diseases with a lower than normal output. We then plot the 100 OE and TE pairs. There are three possible outcomes for the OE versus TE curves. One is that it is linear, where in order to have a 50 % OE we need to inhibit the species by 50 %. The second is a sublinear response, where in order to have an OE of 50 % we need to inhibit the species by more than 50 %. The third is superlinear, where inhibiting the species by less than 50 % would lead to an OE of 50 %.

To compare between species, we choose three TE values: 52%, 91%, and 100% and rank the OE for all the species. The reason we look at different degrees of inhibition of each species and not just when it is 100% inhibited is because it might be better to target a species that results in a higher OE at low levels of inhibition than to target a drug that results in a much higher OE but only when it is inhibited at very high levels. This is because in practice high doses of drug are likely to be toxic.

3.2 Targeting Pairs of Species and Categorizing Them

To identify which pairs of targets works well, we systematically inhibited each of the two species of the pair at 100 different logarithmically spaced concentrations between 10^{-4} and $10^2 \mu M$ with a total of 10^4 different combinations of concentrations. Similar to the targeting of individual species, we maintain a constant amount of the two reversible inhibitors introduced and allow the system to reach steady state with them before simulating the system and obtaining the OEs for all the combinations of the two drug levels.

We then looked at how pairs of drug targets effect the output compared to when each one of the drugs were given alone at equivalent concentrations. To that end, we plotted the first species' TEs, second species' TEs, and OEs for all the 10^4 combinations in a heat plot and categorized the pairs as additive, synergistic, or antagonistic for seven contours of output effect levels of 30%, 50%, 70%, 90%, 99.0%, 99.99%, and 99.999%.

An additive pair means that the two drugs have a linear effect on the output. Graphically, these are the pairs where the overall OE is constant along lines where the total drug concentration is fixed. A synergistic pair is one in which the addition of one of the drugs reduces the amount required of the second drug to obtain an equal overall output effect

compared to a linear combination of the two, requiring an overall lower amount of total drug intake. Graphically, these are the pairs where a higher overall output effect is achieved at some combinations of drugs along some constant drug concentration curves. An antagonistic pair is one where we need a greater total amount of drug to have the same effect on the output than if only one of the drugs was given. Graphically, these are the pairs where a lower overall output effect is achieved at some combinations of drugs along some constant drug concentration curves.

3.3 Features

We scored the species based on the integral of output concentration over time. This is because we saw that the change in amplitude is the same as the change in integral of output concentration over time as the species reached non-periodic steady state. We do not look at other features such as the number of peaks and the average frequency of oscillations as initial work showed that they highly rank species that do not make biological sense. For example, the highly scored negative regulators of NF- κ B and inhibiting a negative regulator would lead to an increase in NF- κ B and not a decrease in it which we want. Furthermore, the results using the number of peaks and average frequency of oscillations features are not consistent with the results obtained from the integral of output concentration over time and amplitude features which make biological sense.

Chapter 4

Model Results

4.1 Disease Model 1: Loss of I κ Bs Function

In diseases that are represented by this model, there are modifications in I κ Bs such that they lose their functionality. In the original healthy model, we start off with initial amounts of I κ Bs that are degraded and consumed by reactions but are also replenished at a constant rate. In order to alter the model to have it represent the disease state with dysfunctional I κ Bs, we change the concentrations of the three I κ Bs to be constant at zero. This is to show that even though I κ Bs are being produced, only dysfunctional ones are. Changing the concentration of transcriptional I κ Bs to be constant at zero produces the exact same results as when we modified the concentrations of I κ Bs. We will use the model in which the concentrations of the three transcriptional I κ Bs are set constant at zero μM .

To know what the effect of this modification of the model on the output nuclear NF- κ B (NF- κ Bn) is, we obtained the area under the curve after running the system for 10^5 secs and saw a 41200 % increase in NF- κ Bn output, $24.16 \mu M$ to $9991.12 \mu M$. This makes sense because we are disrupting the output's inhibitor. For this disease model, the objective is to find drugs that decrease the output of NF- κ Bn.

4.2 Disease Model 2: Inactive IKK

In diseases that are represented by this model, NEMO, a component of IKK, is inactive. In the healthy model we have an initial amount of $0.1 \mu M$ of IKK which gets consumed and degraded over time. In order to alter the model to have it represent the disease state with an inactive IKK, we make IKK be a constant input at $0 \mu M$.

To know what the effect of this modification of the model on the output NF- κ Bn is, we obtained the area under the curve after running the system for 10^5 secs and saw no change in the output levels; In both the healthy model and this altered model the integral of the output is $24.1600 \mu M$. This makes sense because at steady state, IKK and any species complex containing IKK have been completely consumed by degradation or reactions with other species so making them inactive and setting the concentration to zero makes no difference on the output.

There are two possible reasons to why we are not able to capture diseases with an inactive IKK: 1) the model used might not be accurate enough because it might need to represent components of IKK separately or it is not correctly modeling the concentration profile of IKK. 2) NEMO or IKK might be involved in another pathway and the disruption in the other pathway might be the cause of disease.

4.3 Disease Model 3: Constitutively Active IKK

In diseases represented by this model, IKK is constitutively active. In the healthy model we have an initial amount of $0.1 \mu M$ of IKK which gets used up and degraded over time. In order to alter the model to have it represent the disease state with a constitutively active IKK, we make IKK be a constant input at $0.1 \mu M$.

To know what the effect of this modification of the model on the output NF- κ Bn is, we obtained the area under the curve after running the system for 10^5 secs and saw a 24000 % increase in the output (from $24.1600 \mu M$ in the healthy model to $5936.06 \mu M$ in this disease model). This makes sense biologically as having a constant input of the inhibitor to the inhibitors of NF- κ B (I κ Bxs) is equivalent to activating NF- κ B. For this disease model

the objective is to find drugs that decrease the output of NF- κ Bn.

4.4 Disease Models Used in Identifying Targets

Since only disease model 1 (Loss of I κ Bs function) and disease model 3 (Constitutively active IKK) have any effect on the output NF- κ Bn, we will identify individual and pair targets only for them and not disease model 2 (Inactive IKK). Also, since both disease model 1 and disease model 3 lead to an increase in output, we will identify targets that decrease the output.

Chapter 5

Single Target Results

5.1 Single Drug Targets in the Healthy Model

5.1.1 Output Effect - Inhibition Level Profiles for Each Target

The OE vs TE profiles for all species in the healthy model can be found in section B.2 in Appendix B. The species categorization can be seen in figure 5-1.

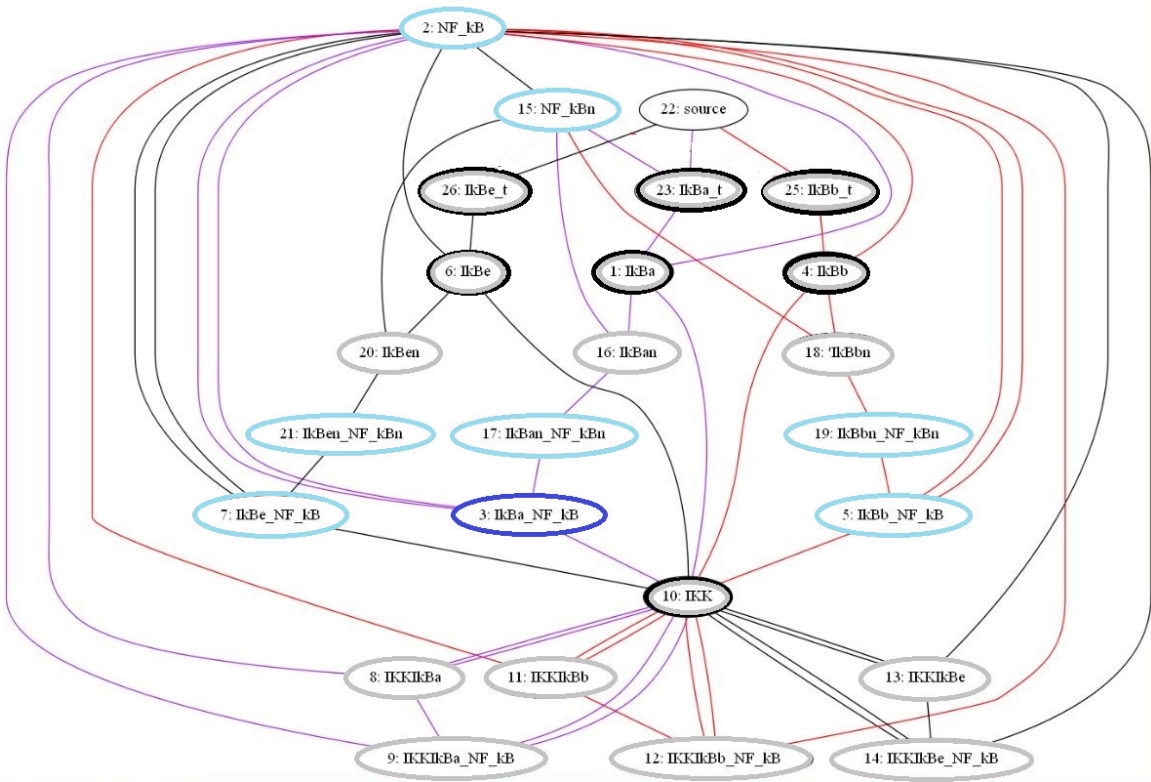


Figure 5-1: Classification of species in the healthy model based on their OE vs TE profiles. Species in dark blue circles have super-linear or linear profiles. Species in light blue circles have sub-linear profiles. Species in grey circles have no effect on the output. Species in black circles get degraded.

5.1.2 Optimal Target and TE level

Figure 5-2 shows the OE for various TEs for all species for the healthy model. The species that achieve an OE > 40

- TE > 30 %: IB_{α} -NF-B (species 3)
- TE > 75 %: IB_{β} -NF-B (species 5)
- TE > 80 %: IB_{ϵ} -NF-B: (species 7)
- TE < 95 %: $IB_{\alpha n}$ -NF-Bn (species 17)
- TE > 99 %: NF-B (species 2), NF-Bn (species 15), $IB_{\beta n}$ -NF-Bn (species 19) , and $IB_{\epsilon n}$ -NF-Bn (species 21)

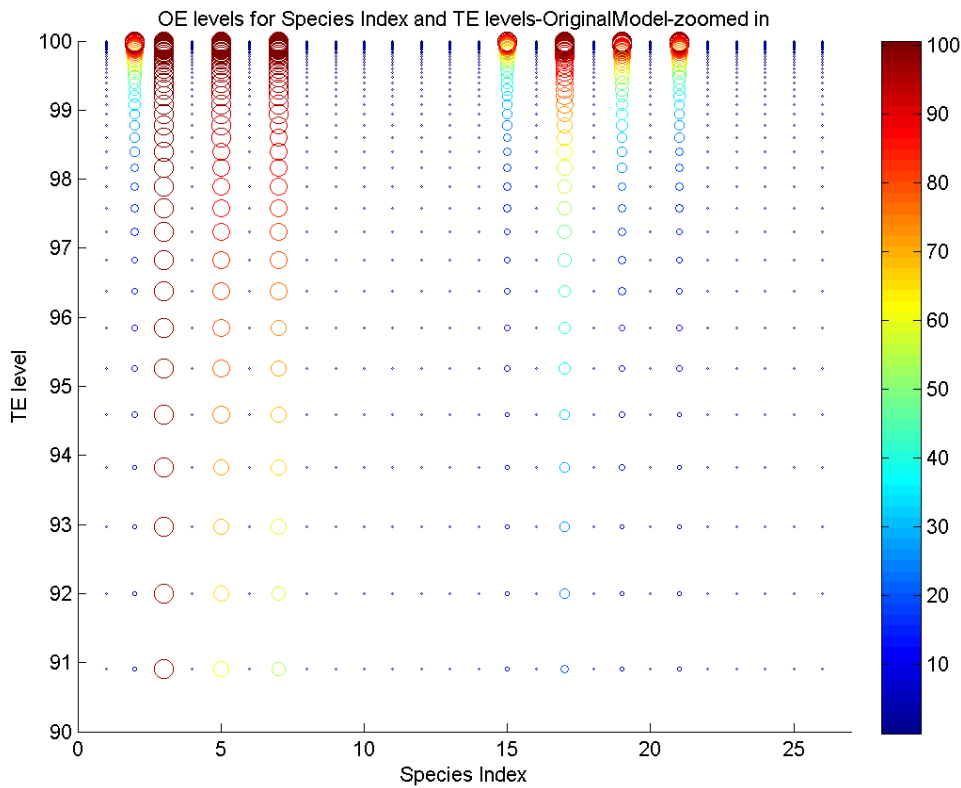
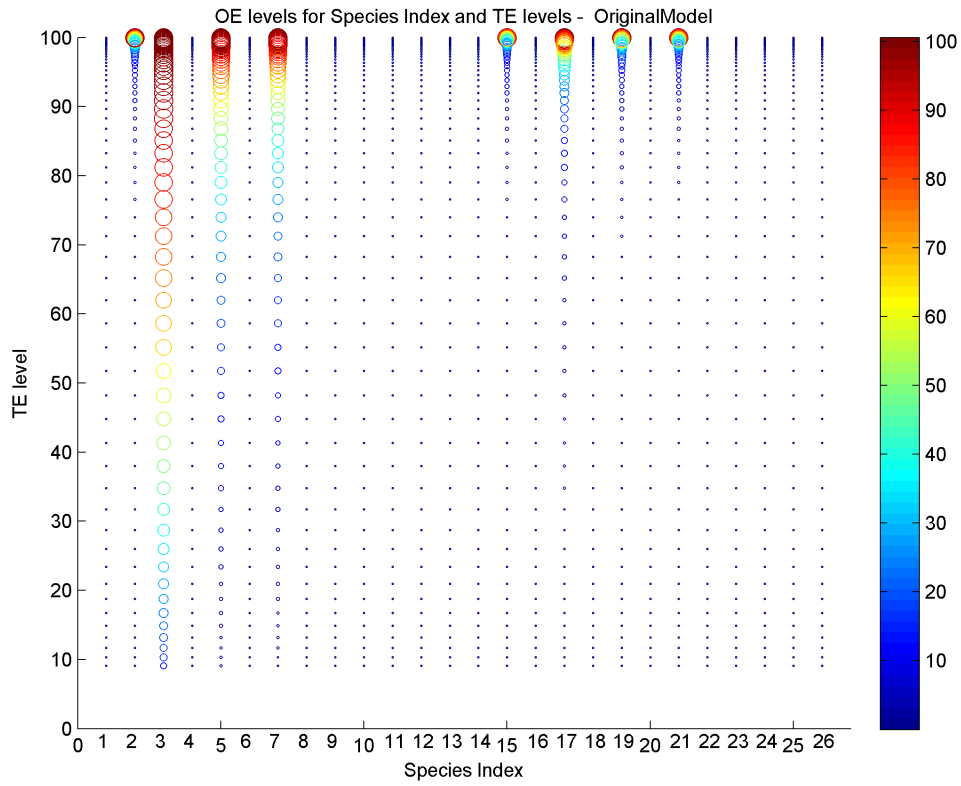


Figure 5-2: OE for various TEs for all species for the original healthy model. The size and color vary according to the OE. Top figure shows all TEs and the bottom figure shows TEs > 90 %.

5.1.3 Optimal Target

The species that achieve and OE level $> 40\%$ with TE ≤ 80 are:

- IB α -NF-B (species 3)
- IB β -NF-B (species 5)
- IB ϵ -NF-B: (species 7)

5.1.4 TE Level Threshold

There is no level threshold that produces OE level $> 40\%$ that works for all species.

5.2 Single Drug Targets in Disease Model 1

5.2.1 Output Effect - Inhibition Level Profiles for Each Target

The OE vs TE profiles for all species in disease model 1 can be found in section B.3 in Appendix B. The species categorization can be seen in figure 5-3.

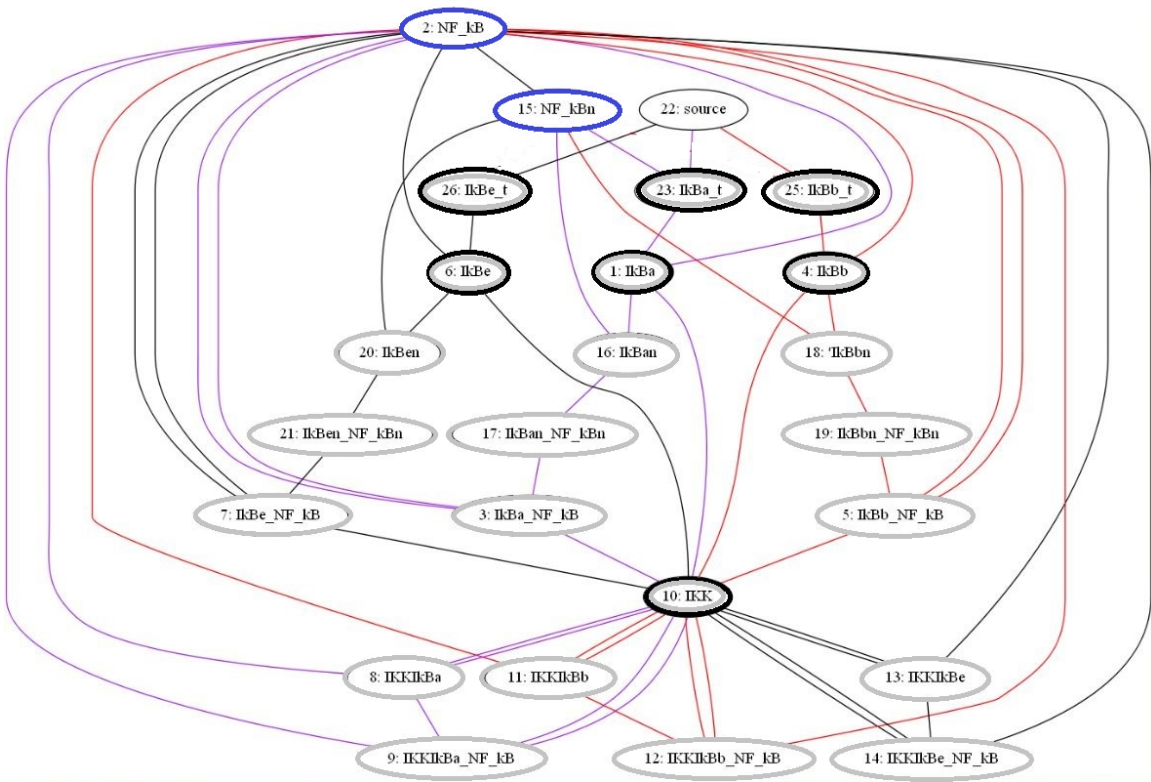


Figure 5-3: Classification of species in disease model 1 based on their OE vs TE profiles. Species in dark blue circles have super-linear or linear profiles. Species in light blue circles have sub-linear profiles. Species in grey circles have no effect on the output. Species in black circles get degraded.

5.2.2 Optimal Target and TE level

Figure 5-4 shows the OE for various TEs for all species for the healthy model. The species that achieve an OE > 40 % are:

- TE > 40 %: NF-Bn (species 15)
- TE very close to 100 %: NF-B (species 2)

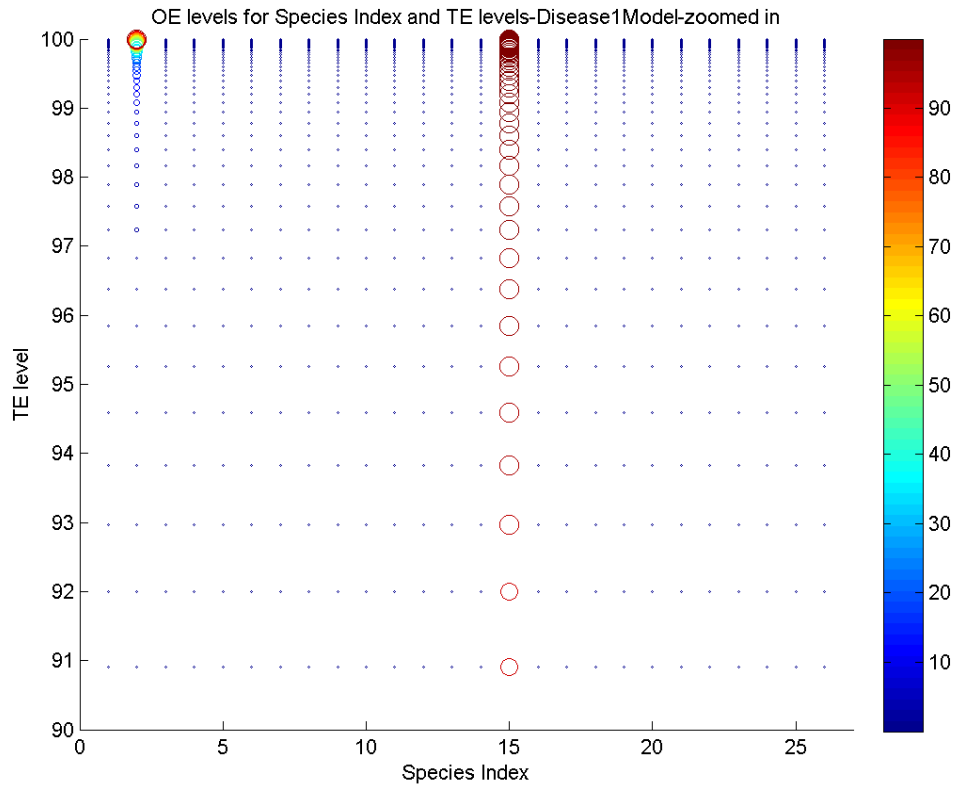
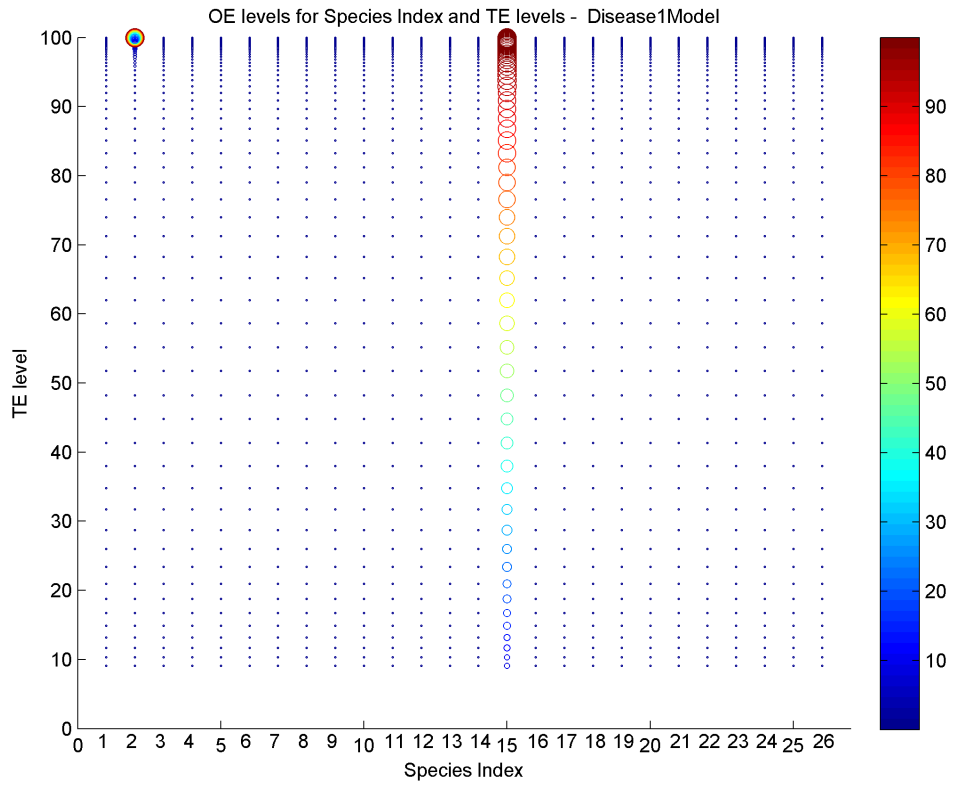


Figure 5-4: OE for various TEs for all species for disease model 1. The size and color vary according to the OE. Top figure shows all TEs and the bottom figure shows TEs > 90 %.

5.2.3 Optimal Target

The species that achieve and OE level $> 40\%$ with TE ≤ 80 :

- NF-Bn (species 15)

5.2.4 TE level Threshold

There is no level threshold that produces OE level > 40 that works for all species

5.3 Single Drug Targets in Disease Model 3

5.3.1 Output Effect - Inhibition Level profiles for each Target

The OE vs TE profiles for all species in the healthy model can be found in section B.4 in Appendix B. The species categorization can be seen in figure 5-5.

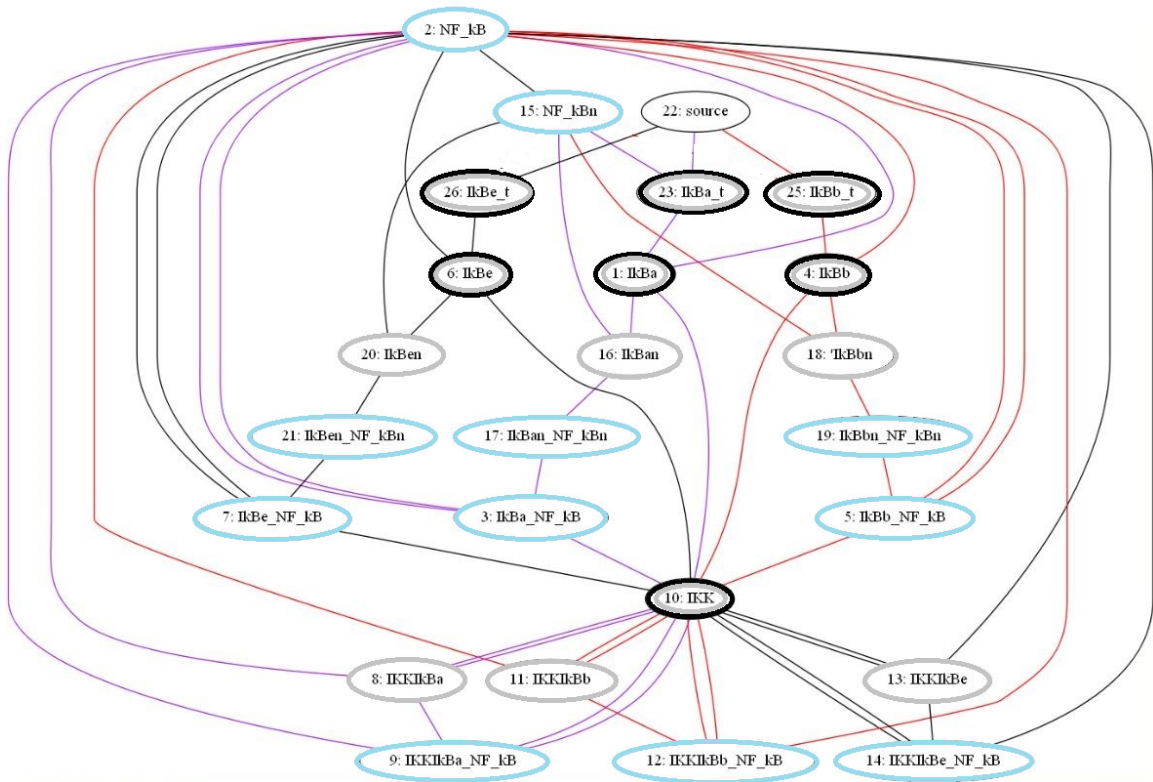


Figure 5-5: Classification of species in the disease model 3 based on their OE vs TE profiles. Species in dark blue circles have super-linear or linear profiles. Species in light blue circles have sub-linear profiles. Species in grey circles have no effect on the output. Species in black circles get degraded.

5.3.2 Optimal Target and TE level

Figure 5-6 shows the OE for various TEs for all species for the disease model 3. The species that achieve an OE > 40 % are:

- TE > 50 %: NF-Bn (species 15)
- TE > 90 %: IB_{α} -NF-B (species 3) and $IKKIB_{\alpha}$ -NF-B (species 9)
- TE > 94 %: $IB_{\alpha n}$ -NF-Bn (species 17)
- TE > 99 %: NF-B (species 2)
- Requires close to 100 % TE: IB_{β} -NF-B (species 5), IB_{ϵ} -NF-B (species 7), $IKKIB_{\beta}$ -NF-B (species 12), $IKKIB_{\epsilon}$ -NF-B (species 14), $IB_{\beta n}$ -NF-Bn (species 19), and $IB_{\epsilon n}$ -NF-Bn (species 21)

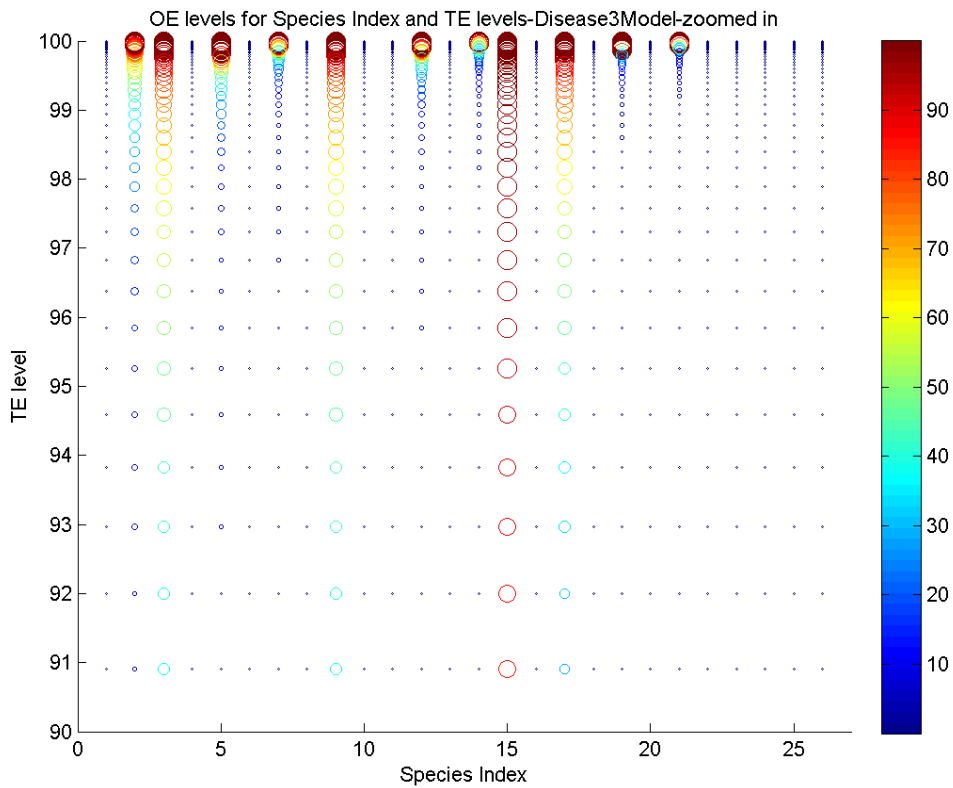
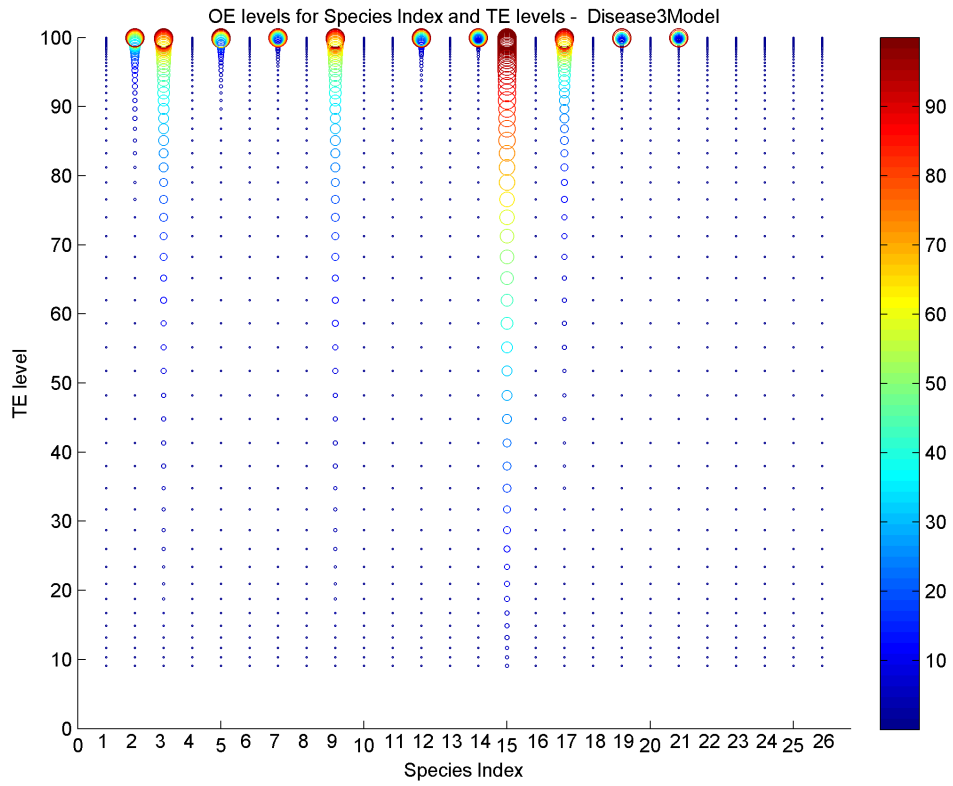


Figure 5-6: OE for various TEs for all species for disease model 3. The size and color vary according to the OE. Top figure shows all TEs and the bottom figure shows TEs > 90 %.

5.3.3 Optimal Target

The species that achieve and OE level $> 40\%$ with TE ≤ 80 :

- NF-Bn (species 15)

5.3.4 TE Level Threshold

There is no level threshold that produces OE level > 40 that works for all species

5.4 Comparison of Single drug targets across models

Figure 5-7 shows the OE for each target across models. Species that reach $> 90\%$ OE regardless of how much inhibition is required that work for at least two of the three models (health model (0), disease 1 model (1), and disease 3 model (3)) are: NF-kB (species 2), $IB\alpha$ -NF-kB (species 3), $IB\beta$ -NF-kB (species 5), $IB\epsilon$ -NF-kB (species 7), NF-kBn (species 15), $IB\alpha$ n-NF-kBn (species 17), $IB\beta$ n-NF-kBn (species 19), and $IB\epsilon$ n-NF-kBn (species 21).

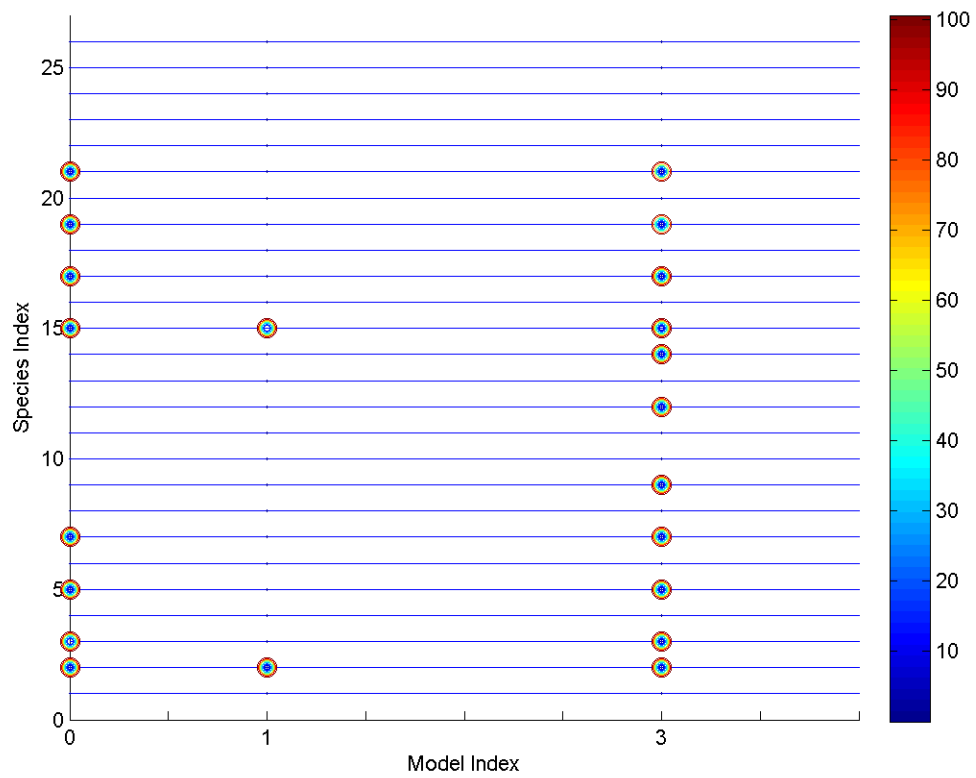


Figure 5-7: OE for each species across models. The size and color vary according to the OE.

Chapter 6

Paired Target Synergy Results

We looked at synergy of pairs at seven different OE levels: 30%, 50%, 70%, 90%, 99.0%, 99.99%, and 99.999% for each of the models.

6.1 Paired Drug Targets in the Healthy Model

Figure 6-1 shows the level of synergy between synergistic pairs at various OE levels. Figure B-5 in Appendix B.5 shows whether each combination of species is synergistic, additive, or antagonistic for the various OE levels. The pairs of species that are synergistic for at least one OE level are all pair combinations of the following species: NF- κ B (2), I κ B α -NF- κ B (3), I κ B β -NF- κ B (5), I κ B ϵ -NF- κ B (7), NF- κ Bn (15), I κ B α n-NF- κ Bn (17), I κ B β n-NF- κ Bn (19), and I κ B ϵ n-NF- κ Bn (21).

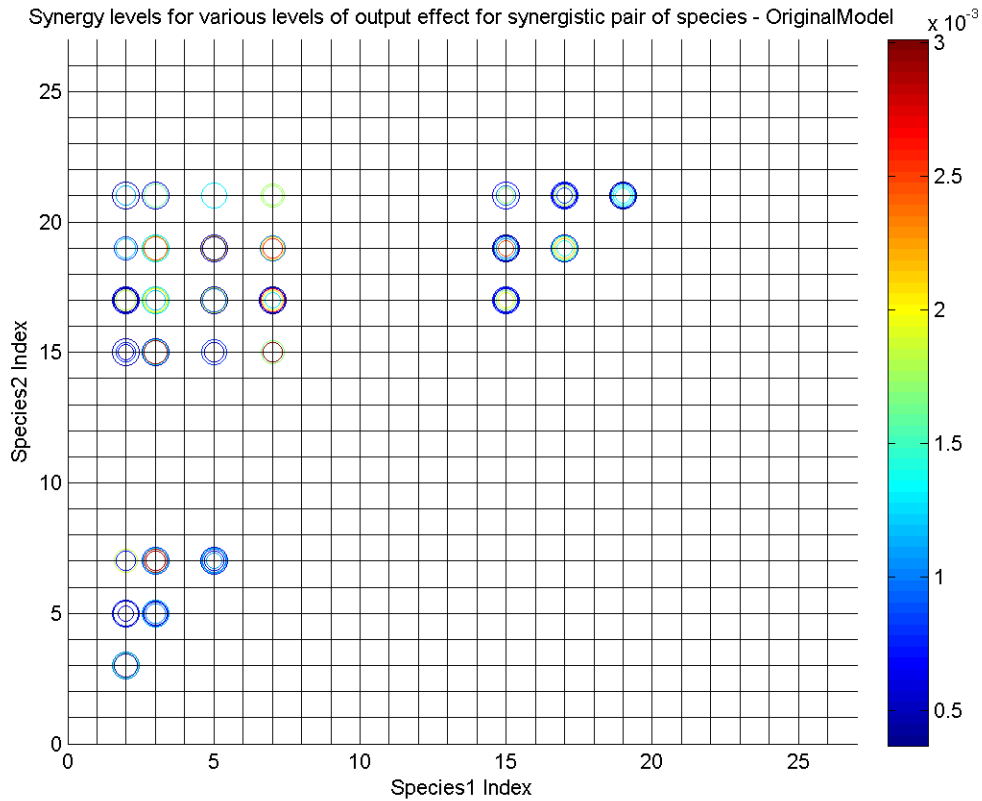


Figure 6-1: Synergy levels for various levels of OE for synergistic pairs of species for the healthy model. The size of the circles varies according to the OE level (but scaled to fit the grids) and the color varies according to the amount of synergism. To give a sense of scale, the pair (7,17) has the following levels of synergism for the seven OE levels: 0.0013, 0.0020, 0.0026, 6.616×10^{-4} , 4.017×10^{-4} , -1.772×10^{-5} (not shown), NaN (not shown).

6.2 Paired Drug Targets in Disease Model 1

Figure 6-2 shows the level of synergy between synergistic pairs at various OE levels. Figure B-6 in Appendix B.5 shows whether each combination of species is synergistic, additive, or antagonistic for the various OE levels. The pairs of species that are synergistic for at least one OE level is only (NF- κ B (2), NF- κ Bn (15)).

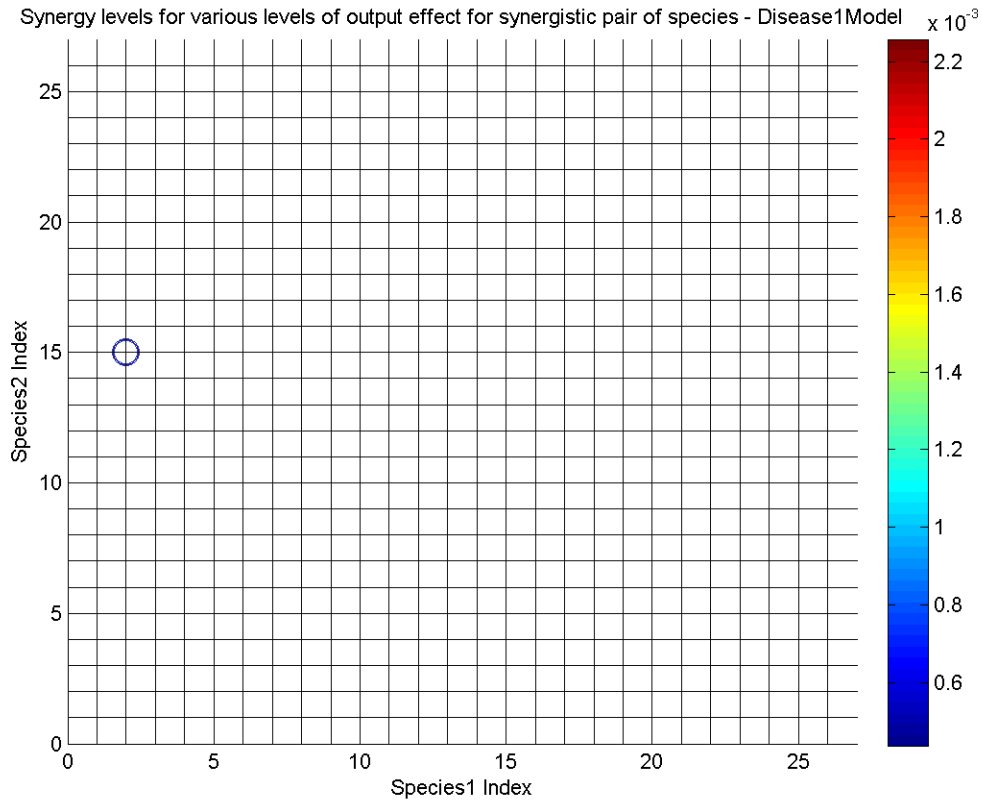


Figure 6-2: Synergy levels for various levels of OE for synergistic pairs of species for the disease model 1. The size of the circles varies according to the OE level and the color varies according to the amount of synergism.

6.3 Paired Drug Targets in Disease Model 3

Figure 6-3 shows the level of synergy between synergistic pairs at various OE levels. Figure B-7 in Appendix B.5 shows whether each combination of species is synergistic, additive, or antagonistic for the various OE levels. The pairs of species that are synergistic for at least one OE level are all pair combinations of NF- κ B (2), I κ B α -NF- κ B (3), I κ B β -NF- κ B (5), I κ B ϵ -NF- κ B (7), IKKI κ B α -NF- κ B (9), IKKI κ B β -NF- κ B(12), IKKI κ B ϵ -NF- κ B(14), NF- κ Bn (15), I κ B α n-NF- κ Bn (17), I κ B β n-NF- κ Bn (19),and I κ B ϵ n-NF- κ Bn (21).

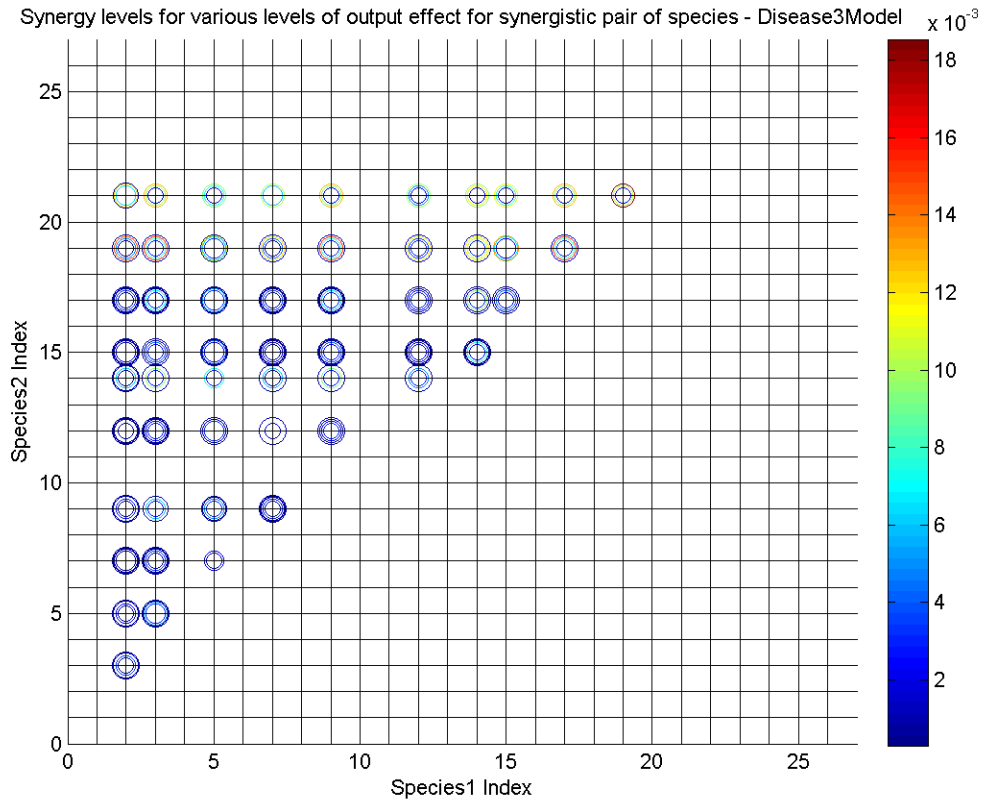


Figure 6-3: Synergy levels for various levels of OE for synergistic pairs of species for the disease model 3. The size of the circles varies according to the OE level and the color varies according to the amount of synergism.

6.4 Paired Drug Targets Across Models

The pairs of species that are synergetic along at least one OE level for at least two of the model are all pair combinations of the following species: $\text{NF-}\kappa\text{B}$ (2), $\text{I}\kappa\text{B}\alpha\text{-NF-}\kappa\text{B}$ (3), $\text{I}\kappa\text{B}\beta\text{-NF-}\kappa\text{B}$ (5), $\text{I}\kappa\text{B}\epsilon\text{-NF-}\kappa\text{B}$ (7), $\text{NF-}\kappa\text{Bn}$ (15), $\text{I}\kappa\text{B}\alpha\text{n-NF-}\kappa\text{Bn}$ (17), $\text{I}\kappa\text{B}\beta\text{n-NF-}\kappa\text{Bn}$ (19), and $\text{I}\kappa\text{B}\epsilon\text{n-NF-}\kappa\text{Bn}$ (21).

Chapter 7

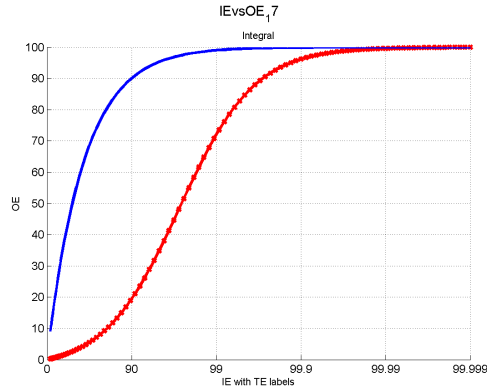
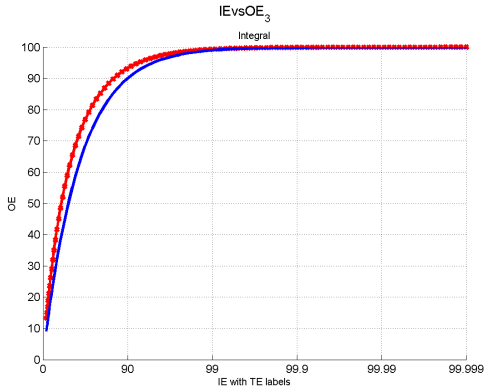
Discussion

7.1 Explanation of Top Scoring Single Targets

In the healthy model, at steady state, all the species are active except for species with IKK. This is because at steady state, all complexes with IKK are completely consumed/degraded. Among the still active species, $I\kappa B\chi$ -t, $I\kappa B\chi$, $I\kappa B\chi n$ have no effect on the output because no matter how much of it is inhibited, there is a constant amount of them being transcribed, thus there is no overall decrease in their amounts in the system when inhibited and thus do not induce any change in $NF-\kappa B n$'s output.

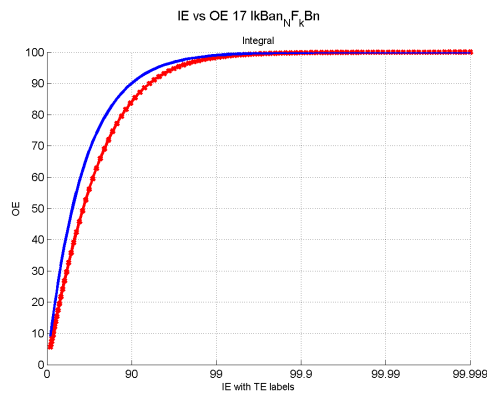
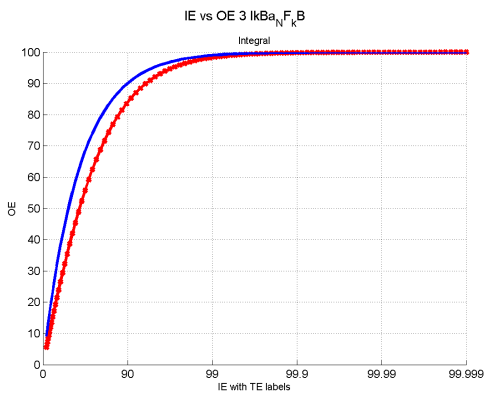
In this model, we see that $I\kappa B\chi$ - $NF-\kappa B$ s are the top scoring species and score much higher than their nuclear counterparts $I\kappa B\chi n$ - $NF-\kappa B$ s. This may be because there is only nuclear export of $I\kappa B\chi n$ - $NF-\kappa B$ s and no nuclear import resulting in a greater steady state concentration of $I\kappa B\chi$ - $NF-\kappa B$ s than of $I\kappa B\chi n$ - $NF-\kappa B$ s. To confirm, we added a nuclear import reaction of $I\kappa B\alpha$ - $NF-\kappa B$ with equal reaction rate as the export. This addition resulted in $I\kappa B\alpha n$ - $NF-\kappa B n$ having similar effectiveness as $I\kappa B\alpha$ - $NF-\kappa B$ as can be seen in figure 7-1.

Also, in this model, $NF-\kappa B$ and $NF-\kappa B n$ are not as effective as $I\kappa B\chi$ - $NF-\kappa B$ and $I\kappa B\chi n$ - $NF-\kappa B n$ as can be seen in figure 7-2. This may be because cytoplasmic and nuclear $NF-\kappa B$ are limited in amount and most of them form complexes with $I\kappa B\chi$ and $I\kappa B\chi n$. $NF-\kappa B$ gets consumed by $I\kappa B\beta$ in reaction # 3, $I\kappa B b$ - $NF-\kappa B$ -association. $NF-\kappa B n$ gets consumed by $I\kappa B\beta n$ in reaction # 23, $I\kappa B b$ - $NF-\kappa B$ -nuclear-association. In both reactions, the forward



(a) OE vs TE profile for $I\kappa B\alpha$ -NF- κB in the healthy model

(b) OE vs TE profile for $I\kappa B\alpha n$ -NF- $\kappa B n$ in the healthy model



(c) OE vs TE profile for $I\kappa B\alpha$ -NF- κB in model with added nuclear import

(d) OE vs TE profile for $I\kappa B\alpha n$ -NF- $\kappa B n$ in model with added nuclear import

Figure 7-1: OE vs TE profiles for cytoplasmic and nuclear $I\kappa B\alpha$ -NF- κB in the healthy model and model with added nuclear import. Adding nuclear import reaction with equal reaction rate as the export causes the nuclear complex to have similar effectiveness as its cytoplasmic counterpart.

reaction rate is greater than the reverse rate. Decreasing the forward rates to be equal to the reverse rates by altering the rate parameters decreases the effectiveness of $I\kappa B\beta$ -NF- κB and $I\kappa B\beta n$ -NF- $\kappa B n$ as can be seen in figure 7-3.

In disease model 1, where $I\kappa B$ s are dysfunctional, the only two species that have any effect on the output are NF- $\kappa B n$ (species 15) and NF- κB (species 2). This is because all the other species are complexes with either IKK or $I\kappa B$ s or both which are both non active/dysfunctional at steady state. Among the two active species, NF- $\kappa B n$ scores much higher than NF- κB , even though this is essentially a two-species linear pathway. The difference in scores is also the case in the other models. The reason for this is because the

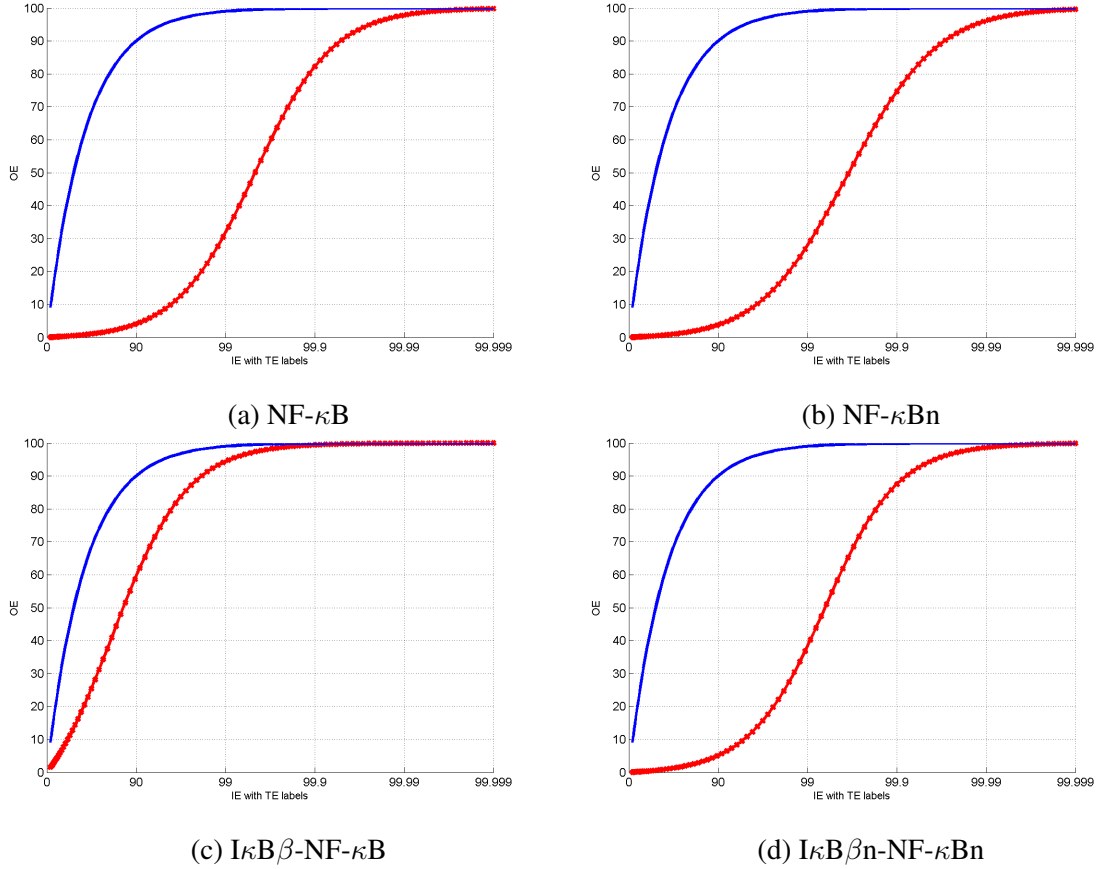


Figure 7-2: OE vs TE for cytoplasmic and nuclear NF- κ B and cytoplasmic and nuclear I κ B β -NF- κ B in the healthy model.

nuclear import rate of NF- κ B is $9 * 10^{-2} s^{-1}$ and the nuclear export rate of NF- κ Bn is $8 * 10^{-5} s^{-1}$ resulting in NF- κ Bn having a much greater steady state concentration than NF- κ B thus having a greater effect when inhibited. Making the import and export rates equal results in NF- κ B and NF- κ Bn having equal effectiveness as can be seen in figure 7-4.

In disease model 3, where IKKs are constitutively active, all the species have some effect on the output except for I κ B χ , I κ B χ n, I κ B χ -t, IKK, and IKKI κ B χ . This is because there is a constant input of IKK and I κ B χ -t (which goes on to become I κ B χ and I κ B χ n).

In this model, I κ B χ -NF- κ Bs do not score as highly as they did in the healthy model. This is because most of the I κ B χ s are used up in forming IKKI κ B χ s with IKK instead of forming I κ B χ -NF- κ B with NF- κ B as the latter is limited by the amount of NF- κ B and at steady state there is a lot more IKK than NF- κ B. To confirm that the decrease in effectiveness of the I κ Bs between the healthy model and disease model 3 is due to having the

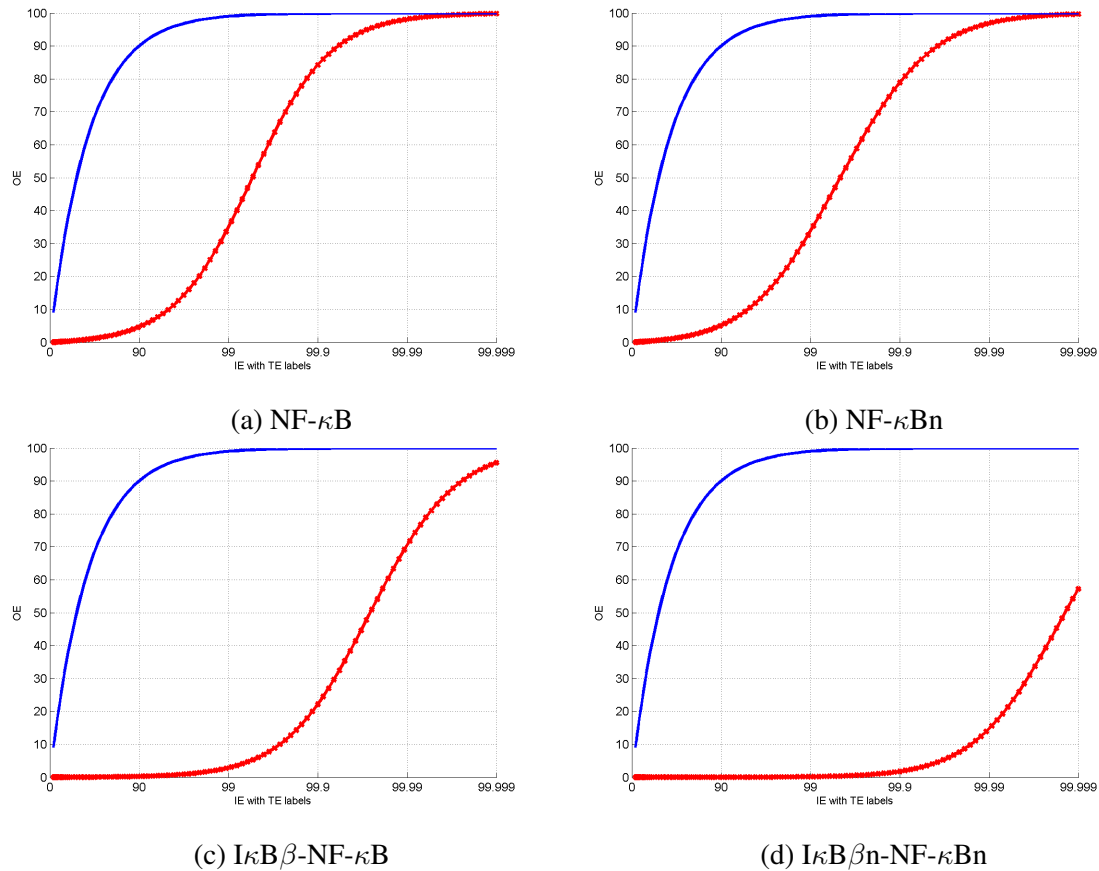
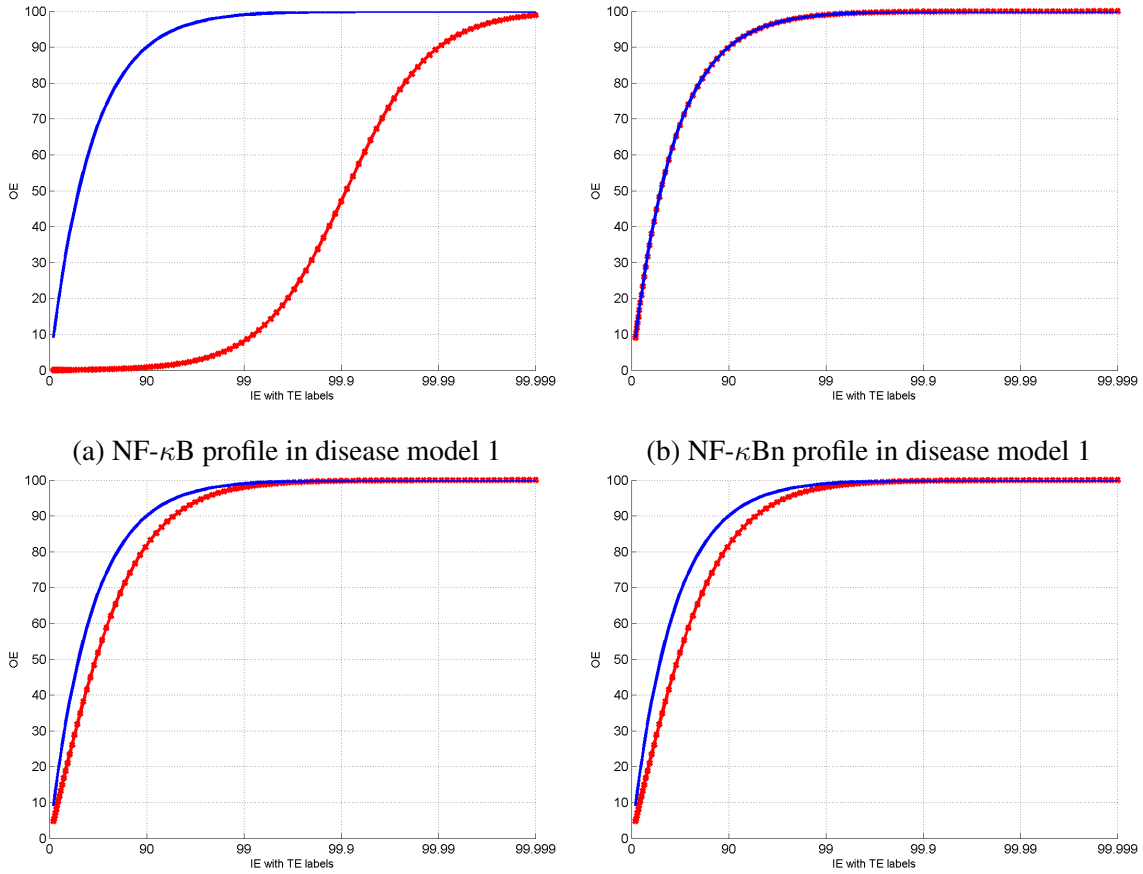


Figure 7-3: OE vs TE profiles for cytoplasmic and nuclear NF- κ B and I κ B β -NF- κ B in the model with equal forward and reverse rates for I κ B β -NF- κ B-association and I κ B β -NF- κ B-nuclear-association.

steady state concentration of IKK being much greater than that of NF- κ B, we altered the model to have IKK be at a constant concentration of $0.0002 \mu M$ roughly equal to the initial concentration of NF- κ B. Decreasing the concentration of IKK results in great increase in OEs of I κ B β -NF- κ Bs (figure 7-5) confirming our hypothesis.

Also, in this model the OE of NF- κ B is a lot greater than its effect in the healthy model. This could also be attributed to the same cause as before, namely, more of the I κ B β s are forming complexes with IKK instead of with NF- κ B. This causes there to be more free NF- κ B/NF- κ Bn in the system to be inhibited. The same alteration of decreasing the concentration of IKK results in a large decrease in the OE of NF- κ B as can be seen in figure 7-6.

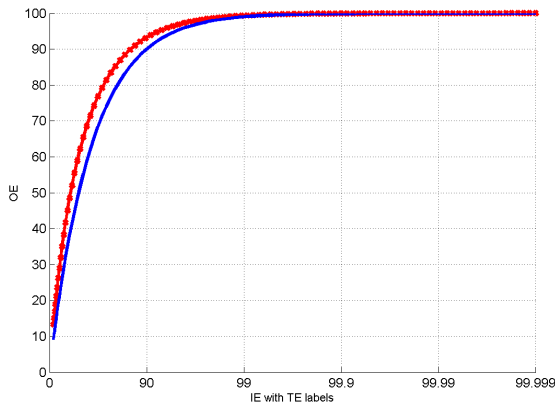
Overall, we can say that only species that are limited in production have any effect on



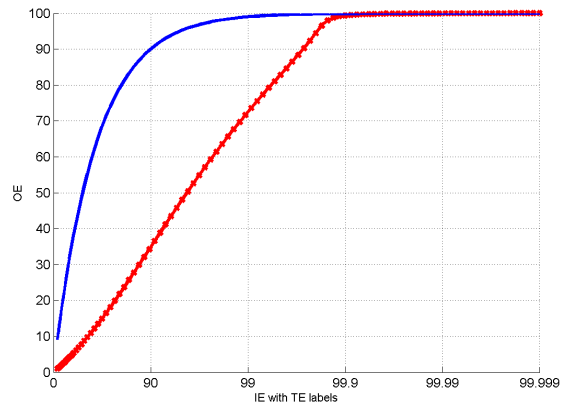
(a) NF- κ B profile in disease model 1 (b) NF- κ Bn profile in disease model 1
(c) NF- κ B profile in model with equal nuclear import and export rates of NF- κ B (d) NF- κ Bn profile in model with equal nuclear import and export rates of NF- κ B

Figure 7-4: OE vs TE profiles of cytoplasmic and nuclear NF- κ B in disease model 1 and in a model with equal nuclear import and export rates of NF- κ B. Modifying the import and export rates to be equal causes the profiles of the cytoplasmic and nuclear NF- κ B to be similar.

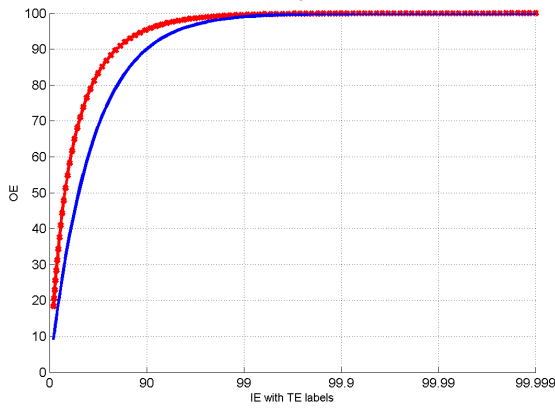
the output and any species that are constantly being produced have no effect. Also, among the species that are limited in production, the ones with greater steady state concentration have a greater effect.



(a) Healthy model

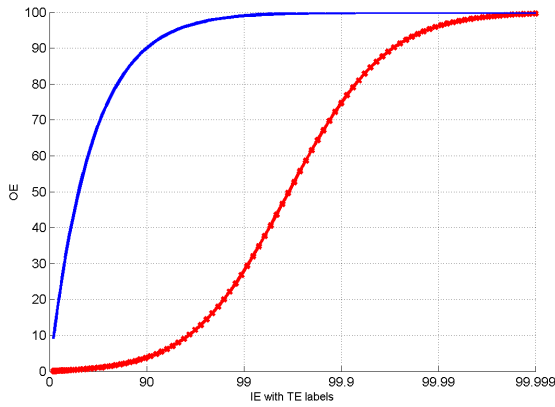


(b) Disease model 3

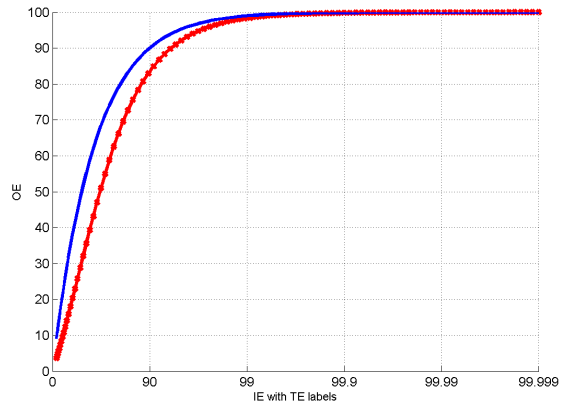


(c) Model with decreased concentration of IKK

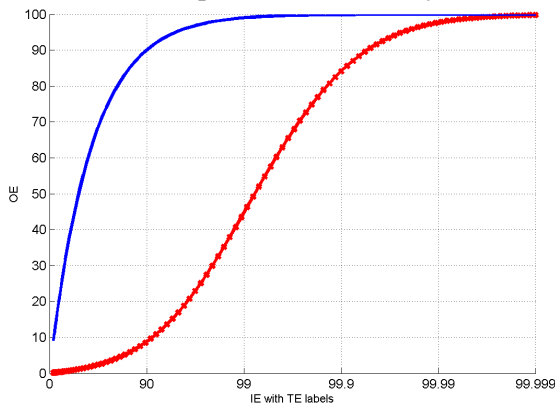
Figure 7-5: $I\kappa B\alpha$ -NF- κB profile in the healthy model, disease model 3, and model with decreased IKK concentration. $I\kappa B\alpha$ -NF- κB is less effective in disease model 3 than in the healthy model. Decreasing the concentration of IKK increases effectiveness of $I\kappa B\alpha$ -NF- κB .



(a) NF- κ Bn profile in the healthy model



(b) NF- κ Bn profile in disease model 3



(c) NF- κ Bn profile in model with decreased concentration of IKK

Figure 7-6: NF- κ Bn profiles in the healthy model, disease model 3, and model with decreased IKK concentration. The effectiveness of NF- κ Bn is greater in disease model 3 than it is in the healthy model. Decreasing the concentration of IKK decreases the effectiveness of NF- κ Bn

7.2 Why does the output, NF- κ Bn, not have a linear profile?

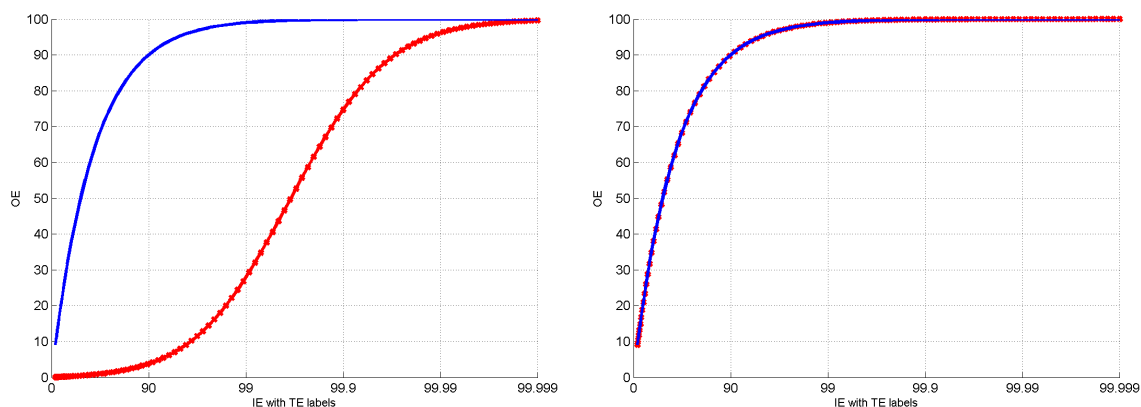
One key observation we see is that the OE vs TE profile for the output, nuclear NF- κ B (NF- κ Bn, species # 15), is not linear. We expect a linear profile for the output because we are inhibiting and measuring the change for the same species. Understanding the reactions and the species NF- κ Bn is directly involved in led us to come up with three possible explanations to to this observation. These are: (1) there are competing reactions with the added inhibitor, (2) NF- κ Bn is involved in the synthesis of one of its inhibitors, I κ B α , (3) there is a limitless amount of its inhibitors in the system and only a limited amount of NF- κ Bn.

NF- κ Bn is directly involved in the following sets of reactions: (1) NF- κ B-nuclear-import/export ($k_i = 1.125 * 10^3$), (2) I κ B χ -NF- κ B nuclear-association/dissociation ($k_i = 1 * 10^{-3} \mu M$), (3) I κ B α -Inducible-mRNA-synthesis ($k = 0.0165 \mu M^{-1} s^{-1}$). The inhibition constant that we used was $10^{-3} \mu M$. The smaller the dissociation constant the stronger the reaction is and the less free NF- κ Bn there is. The inhibition constant we used is greater or equal in strength to its competitors. To truly confirm whether competition is the reason for this observation, we used a stronger inhibitor with an inhibition constant of $10^{-6} \mu M$ and saw that using a much stronger inhibitor did not make the NF- κ Bn OE vs TE profile any more linear. Thus, it is not competition that caused this non-linearity.

To see if the reason for this non-linearity is because NF- κ Bn is involved in the synthesis of I κ B α (one of its inhibitors) via reaction # 28 (NF- κ Bn + NF- κ Bn \rightarrow I κ B α -t + NF- κ Bn + NF- κ Bn), we removed the reaction from the model. This did not make the profile linear.

The last possible explanation for why the output itself has a nonlinear profile is that there is a limitless amount of its inhibitors (I κ B α , I κ B β , and I κ B ϵ) but only a limited amount of NF- κ Bn. To test this hypothesis, we modified the system and removed the constant input of inhibitor by setting the source to zero. In this modification the output did have a linear profile. Therefore, the constant amount of I κ Bs is the reason for the non-linearity. This reasoning is reinforced by the fact that in disease model 1, where the I κ Bs are dysfunctional, result in a linear profile, whereas in the healthy model and disease model 3 do not result in a linear profile. Figure 7-7 shows the OE vs TE profile for the output in

disease model 1 and the healthy model.



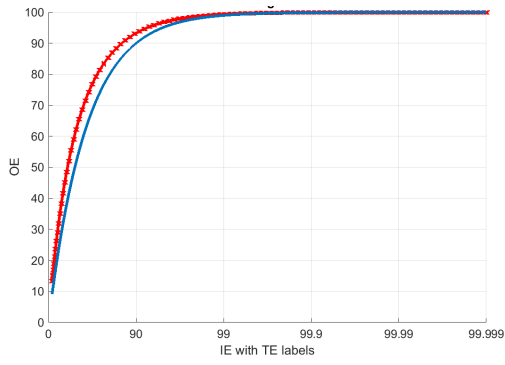
(a) OE vs TE profile of NF- κ B in the healthy model (b) OE vs TE profile of NF- κ B in disease model 1

Figure 7-7: OE vs TE profile for the output NF- κ B in the healthy model and disease model 1. The profile is sub-linear in the healthy model and linear in disease model 1.

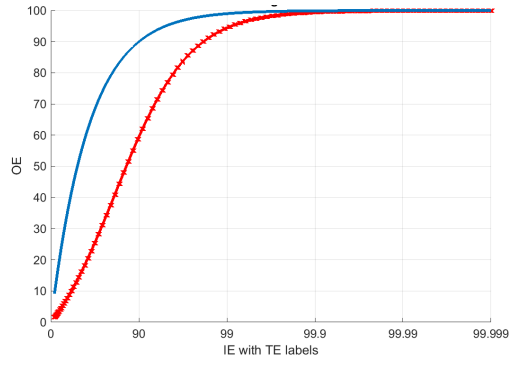
7.3 Why are alpha isoforms better drug targets than the beta and epsilon isoforms?

Another key observation we see is that alpha isoforms are better drug targets than the beta and epsilon isoforms. This is true in both the healthy model and disease model 3, and is not applicable to disease model 1 because the I κ Bs are dysfunctional causing all species with I κ Bs to be dysfunctional. The biggest differences in scores can be observed in the I κ B α -NF- κ B species.

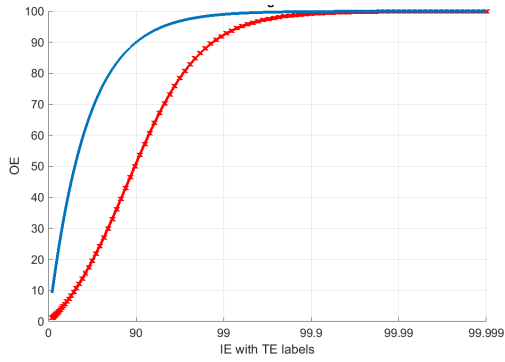
Figures 7-8 and 7-9 show the OE vs TE profiles for the three isoforms in the healthy model and disease model 3 respectively. In the healthy model, I κ B α -NF- κ B (species 3) only requires a TE of about 30 % to achieve an OE level of 40 %; I κ B β -NF- κ B (species 5) and I κ B ϵ -NF- κ B (species 7) require TEs greater than 75 % to achieve the same OE level. Similarly, in disease model 3, I κ B α -NF- κ B can achieve an OE level of 40 % with a TE of 90 %, whereas both I κ B β -NF- κ B and I κ B ϵ -NF- κ B require a TE close to 100 % to achieve the same OE level.



(a) $I\kappa B\alpha$ -NF- κB



(b) $I\kappa B\beta$ -NF- κB



(c) $I\kappa B\epsilon$ -NF- κB

Figure 7-8: OE vs TE profiles for $I\kappa B\alpha$ -NF- κB , $I\kappa B\beta$ -NF- κB , and $I\kappa B\epsilon$ -NF- κB using the original healthy model.

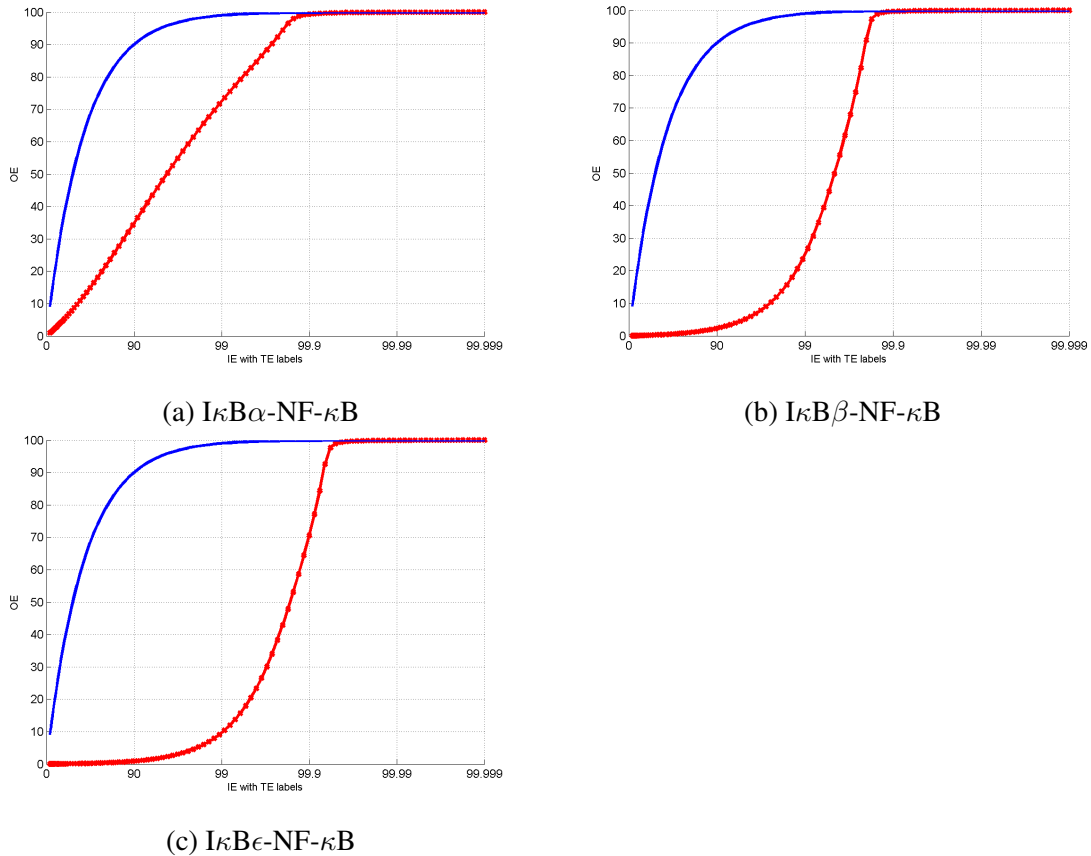


Figure 7-9: OE vs TE profiles for $I\kappa B\alpha$ -NF- κ B, $I\kappa B\beta$ -NF- κ B, and $I\kappa B\epsilon$ -NF- κ B using disease model 3.

There are two major differences between the alpha and the beta/epsilon isoforms in the pathway. The first is that the alpha isoform of $I\kappa B$ -t is the only isoform that gets synthesized inducibly by NF- κ Bn (reaction # 28). The second is that $I\kappa B\alpha$ -t is synthesized at a greater rate than either $I\kappa B\beta$ -t or $I\kappa B\epsilon$ -t. In order to know which of the two explains the gap in scores the best, we made two alterations to the healthy model. In the first, we eliminated the $I\kappa B\alpha$ inducible mRNA synthesis reaction. In the second, we altered the model so that all the isoforms are synthesized at the same rate. We chose a rate of $1.54 * 10^{-6} \mu M^{-1} s^{-1}$ as the synthesis rate of all three isoforms (the same as the original synthesis rate of $I\kappa B\alpha$ -t).

Eliminating the $I\kappa B\alpha$ inducible mRNA synthesis reaction does not reduce the gap between the three different isoforms and hence is not the reason for the differences in scoring. This makes sense because the majority of $I\kappa B\alpha$ -t is synthesized constitutively via the "con-

stitutive $I\kappa B\alpha$ - mRNA synthesis" reaction and not from the inducible synthesis $NF-\kappa Bn + NF-\kappa Bn \rightarrow I\kappa B\alpha - t + NF-\kappa Bn + NF-\kappa Bn$ as the latter depends on the amount of $NF-\kappa Bn$, which is limited, while there is constant input of $I\kappa B\alpha-t$ from the source. Also, it would not have explained why beta isoforms score better than the epsilon ones.

Modifying the synthesis rates of $I\kappa B\alpha-t$, $I\kappa B\beta-t$, and $I\kappa B\epsilon-t$ to be the same completely eliminated the gap between the three isoforms of $I\kappa Bx-NF-\kappa B$ as can be seen in figure 7-10. This confirms the hypothesis that the difference in synthesis rates of the three isoforms is the main reason for the differences in their scores.

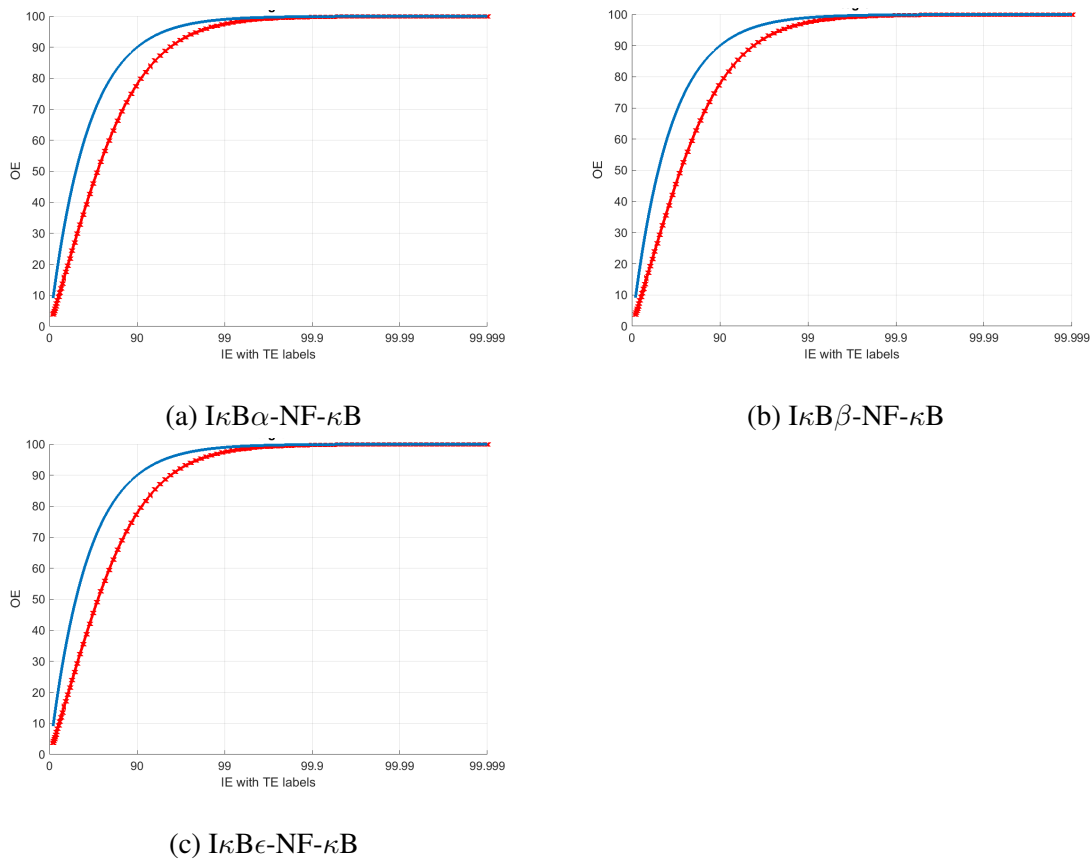


Figure 7-10: OE vs TE profiles for $I\kappa B\alpha-NF-\kappa B$, $I\kappa B\beta-NF-\kappa B$, and $I\kappa B\epsilon-NF-\kappa B$ using model with equal transcription rates of $I\kappa B\alpha-t$, $I\kappa B\beta-t$, and $I\kappa B\epsilon-t$.

The varying rates of transcription could be attributed to the sizes of the proteins. The molecular weight of the alpha, beta, and epsilon isoforms of $I\kappa Bx$ are 35,609 Da, 37,771 Da, and 52,864 Da [16], respectively. The synthesis rates of these three proteins decrease with the increase in molecular weight. $I\kappa B\epsilon$, the heaviest, is the slowest to get transcribed

and $I\kappa B\alpha$, the lightest, is the fastest to get transcribed.

Having the synthesis rates of all three isoforms equal made all three $I\kappa B_X$ -NF- κ B isoforms have the same effect on the output, however, at the same time it greatly decreased the impact of $I\kappa B\alpha$ -NF- κ B (the TE required to achieve an OE of 40% increased from $\approx 30\%$ to $\approx 60\%$). A possible way of looking at the pathway which will explain the decrease in $I\kappa B\alpha$ -NF- κ B's efficacy is looking at it as having three parallel paths with each path's capacity being proportional to the transcription rate of that isoform. This simplified explanatory model is illustrated in figure 7-11.

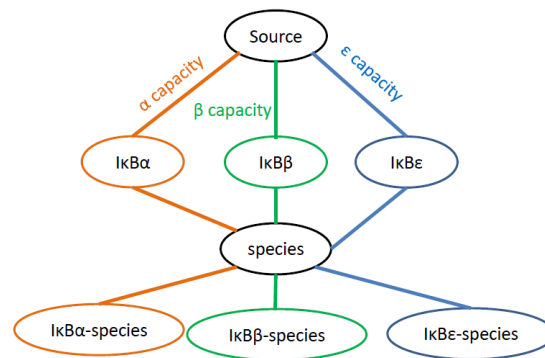


Figure 7-11: A simplified view of the NF- κ B pathway where there are three parallel paths corresponding to the three isoforms each with its own capacity.

To confirm that this view of the pathway is reasonable, we asserted that the model exhibits the following two behaviors: (1) increasing the capacity of the other paths would decrease the effectiveness of the path in question, (2) decreasing the number of parallel paths would increase the effectiveness of the path in question.

We already saw when comparing figures 7-8 and 7-10 that increasing the transcription rate (the "capacity") of the beta, and epsilon isoforms of $I\kappa B_X$, decreases the effectiveness of $I\kappa B\alpha$. To confirm that the number of parallel paths effects the impact of the path being examined, we altered the pathway such that the epsilon path is removed and we only have the alpha and beta paths with the same capacity (by having the synthesis rates equal). If our hypothesis is true we would expect to see an increase in the effectiveness of both the alpha and beta targets. Figure 7-12 shows the OE vs TE of both $I\kappa B\alpha$ -NF- κ B and $I\kappa B\beta$ -NF- κ B with the alterations specified and we indeed see an increase in effectiveness.

Having confirmed that the view of parallel paths is a reasonable one, we can now see

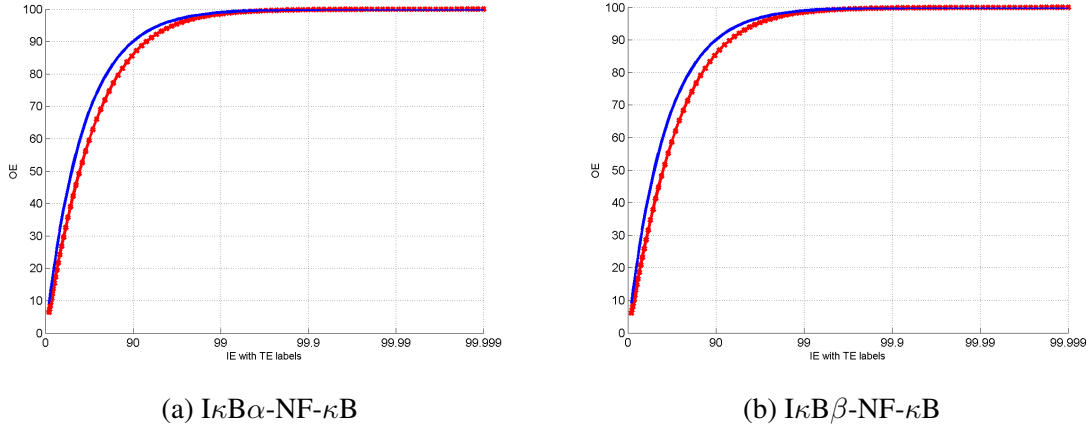


Figure 7-12: OE vs TE profiles for $I\kappa B\alpha$ -NF- κB and $I\kappa B\beta$ -NF- κB using model with equal transcription rates of $I\kappa B\alpha$ -t and $I\kappa B\beta$ -t but without $I\kappa B\epsilon$ -t.

that the reason the impact of $I\kappa B\alpha$ -NF- κB decreased when we increased the transcription rate of $I\kappa B\beta$ -t and $I\kappa B\epsilon$ -t is because even though we are restricting the α path the same percentage as before there is now more capacity in the β and ϵ paths to compensate for that requiring a greater restriction to achieve the same OE.

7.4 Combination of Targets Classification

We classified all combinations of targets as additive, synergistic, or antagonistic. An additive pair is one in which a linear combination of the two drug concentrations leads to the same overall effect on the output. A synergistic pair is one in which the addition of one of the drugs reduces the amount required of the second drug to obtain an equal overall output effect compared to a linear combination of the two, requiring an overall lower amount of total drug intake. An antagonistic pair is one where we need a greater total amount of drug to have the same effect on the output than if only one of the drugs was given. Figures 6-1, 6-2, and 6-3 in section 6.1 show only the synergistic pairs in the healthy model, disease model 1, and disease model 3 respectively. Figures B-5, B-6, and B-7 in section B.5 show the classification of all pairs.

The combination of targets that are categorized as synergistic are combinations of targets that individually have some effect on the output when inhibited. Furthermore, all effective targets (super-linear, linear, and sub-linear) are synergistic with each other for most

of the OE contours. This is regardless of whether the two targets are isoforms of the same species such as $I_{\kappa}B_{\alpha}$ -NF- κ B and $I_{\kappa}B_{\beta}$ -NF- κ B, or different species such as $I_{\kappa}B_{\alpha}$ -NF- κ B and $IKKI_{\kappa}B_{\alpha}$ -NF- κ B. Furthermore, there does not seem to be a trend in the level of synergy between targets. Targets that are isoforms of the same species are no more synergistic than other pairs and combinations of targets that are both super-linear or linear are no more synergistic than pairs between super-linear/linear and sub-linear targets or sub-linear and sub-linear targets. Also, the level of synergism does not seem to depend on the OE contour levels.

The combinations of pairs that are categorized as antagonistic and additive are the combinations of targets with one of them having some effect on the output and the other having no effect. The ones that are categorized as antagonistic are the ones in which the first target has some effect on the output when inhibited but the second has no effect. An example of an antagonistic pair is NF- κ B and $I_{\kappa}B_{\epsilon}$ -NF- κ Bn (in disease model 1). NF- κ B has sub-linear effect on the output but $I_{\kappa}B_{\epsilon}$ -NF- κ Bn has no effect. The ones that are categorized as additive are ones in which the first target has no effect on the output and the second has some effect, very similar to pairs categorized as antagonistic but reversed. An example of an additive pair is $I_{\kappa}B_{\alpha}$ and NF- κ B (in disease model 1).

The remaining combinations of targets that do not fall into any of the three categories are the ones with both species not having any effect on the output. An example is the pair $IKKI_{\kappa}B_{\alpha}$ and $IKKI_{\kappa}B_{\epsilon}$ -NF- κ B (in the healthy model).

In the thesis work of Nirmala Paudel [15], she had categorized combinations of targets in the EGFR pathway and found a general trend for the synergistic combinations, which is that synergism happens between binding partners. Our finding that synergism happens when both species have some effect on the output includes binding partners but also include non-binding partners. The thesis work also found a general trend for antagonistic pairs. Namely, she found that generally antagonism occurs between one of the binding partners and the downstream complex it forms. Our findings do not support this trend as we found that if the downstream complex and one of the binding partners both have some effect on the output then they are synergistic. The difference in the trends found may be because they are pathway/model dependent.

7.5 Comparison of Identified Drug Targets to Existing Ones

Overall, we can categorize the species in the pathway as either having some effect on the output (nuclear NF- κ B or "NF- κ Bn") or not having any. Specifically, any species that is not constantly being produced and is active at steady state has an effect on the output.

In disease model 1, where I κ Bs are dysfunctional, only two species are effective targets: cytoplasmic NF- κ B, or "NF- κ B", and nuclear NF- κ B, or "NF- κ Bn". The effective targets in the healthy model include the two effective species in disease model 1 but also include cytoplasmic I κ Bs complexes with cytoplasmic NF- κ B (I κ B α -NF- κ B, I κ B β -NF- κ B, and I κ B ϵ -NF- κ B) and nuclear I κ Bs with nuclear NF- κ B (I κ B α n-NF- κ Bn, I κ B β n-NF- κ Bn, and I κ B ϵ n-NF- κ Bn). The effective targets in disease model 3, where IKK is constitutively active, include all the effective targets in the healthy model in addition to complexes of I κ B-NF- κ B with IKK (IKKI κ B α n-NF- κ Bn, IKKI κ B β n-NF- κ Bn, and IKKI κ B ϵ n-NF- κ Bn). The optimal drug targets depend on the model used. For the healthy model, we found it to be I κ B α -NF- κ B, I κ B β -NF- κ B, and I κ B ϵ -NF- κ B; for disease model 1 and 3 it is NF- κ Bn.

There have been many species and reactions in the NF- κ B pathway that have been identified as NF- κ B inhibitors. Most of them are upstream of IKK and NF- κ B and are not included in our model. Examples of such targets are TNF-Receptors [6], TRAF6 binding [17], activation of NF- κ B [18], etc. Among the ones identified and are included in our model are I κ B α [19], I κ B β [5], IKK [4], and NF- κ B [20]. Specifically, it has been found that upregulation of I κ B α and I κ B β and the downregulation of IKK and NF- κ B by added drugs lead to the inhibition of NF- κ Bn.

NF- κ B being an effective drug target is consistent with our findings where in all the models inhibiting cytoplasmic NF- κ B leads to the inhibition of nuclear NF- κ B. However, our findings are not consistent with previous ones for I κ B α , I κ B β , and IKK. Specifically, we have found that I κ B α , I κ B β , and IKK have no effect on the output NF- κ Bn. This inconsistency is because in our models whenever a species gets transcribed, as in the case of I κ B α and I κ B β , it is modeled as having an infinite supply where in reality it doesn't. In

the case of IKK, in the healthy model and disease model 1, it is modeled as only having an initial amount that dies out when in reality it might be produced at other times. And in disease model 3, it is modeled as having a constant value and in reality that might not always be the case.

There are targets that we found to be effective but have not been previously identified. These include $I\kappa B\alpha$ -NF- κ B, $I\kappa B\beta$ -NF- κ B, $I\kappa B\epsilon$ -NF- κ B, $I\kappa B\alpha$ n-NF- κ Bn, $I\kappa B\beta$ n-NF- κ Bn, and $I\kappa B\epsilon$ n-NF- κ Bn; and specifically in disease model 3, $IKKI\kappa B\alpha$ n-NF- κ Bn, $IKKI\kappa B\beta$ n-NF- κ Bn, and $IKKI\kappa B\epsilon$ n-NF- κ Bn. One reason they might not have been experimentally identified is because protein complexes are harder to physically inhibit than individual ones.

Chapter 8

Conclusion

In this thesis, we altered the healthy NF- κ B model by Kell et al. [9] to reflect what happens in three different disease states. We restricted the alterations to species/reactions that are included in the model used and gave examples of diseases represented by each of the disease models. The different disease models were ones with loss of I κ Bs function, inactive IKK, and constitutively active IKK.

For the disease models that increased or decreased the amount of nuclear NF- κ Bn (NF- κ Bn) relative to what is produced in the healthy model, we exhaustively scored the species based on how much change in the amount of NF- κ Bn produced they caused when inhibited. We performed the same analysis on the healthy model in order to get an overall picture of which species have control over the amount of NF- κ Bn produced. We found that in all the models analysed, all the species either decreased the output when inhibited or had no effect. We also found that very few species are effective at low levels of inhibition but many are effective at extremely high levels of inhibition. The exception is in the model with loss of I κ Bs function in which we found that only one species other than the output, NF- κ Bn, had any effect and that is the cytoplasmic NF- κ B. The species that are effective at low levels of inhibition in the healthy model are the three cytoplasmic I κ B-NF- κ B complexes; and in disease model 1 and 3 it is the nuclear NF- κ B.

We then provided explanations to why certain species score better than others and explanations to two key observations: 1) why does the output, NF- κ Bn, not have a linear profile? 2) why are alpha isoforms better drug targets than the beta and epsilon isoforms?

We also categorized all combinations of targets as synergistic, antagonistic, or additive and found that all species that have some effect on the output are synergistic with one another. Antagonistic pairs were found to be ones where one of the targets is effective and the other target has no effect when inhibited individually.

Finally, we compared the targets we found to be effective to previously identified drug targets. We found that existing drug targets are restricted to individual proteins and not complexes, though we found that complexes generally scored better than others. The inconsistency is because we only considered signal propagation and not structural limitations when scoring species.

Also, our model only includes the interactions between the species most downstream of the pathway and does not include upstream species and reactions starting with the surface receptors. Expanding the model to include upstream species and their interactions would allow one to model many other different diseases that are caused by alterations in those upstream species and reactions.

Appendix A

Tables

A.1 Healthy NF- κ B Model Species and Their Initial Concentrations.

Species index	Species name	Initial concentration (μ M)
1	$I\kappa B\alpha$	0.189664
2	NF- κ B	0.000251
3	$I\kappa B\alpha$ -NF- κ B	0.083333
4	$I\kappa B\beta$	0.021635
5	$I\kappa B\beta$ -NF- κ B	0.008305
6	$I\kappa B\epsilon$	0.015436
7	$I\kappa B\epsilon$ -NF- κ B	0.005925
8	IKK $I\kappa B\alpha$	0
9	IKK $I\kappa B\alpha$ -NF- κ B	0
10	IKK	0.1
11	IKK $I\kappa B\beta$	0
12	IKK $I\kappa B\beta$ -NF- κ B	0
13	IKK $I\kappa B\epsilon$	0
14	IKK $I\kappa B\epsilon$ -NF- κ B	0

15	NF- κ Bn	0.000217
16	I κ B α n	1.89E-01
17	I κ B α n-NF- κ Bn	1.43E-03
18	I κ B β n	1.65E-02
19	I κ B β n-NF- κ Bn	0.000314
20	I κ B ϵ n	1.18E-02
21	I κ B ϵ n-NF- κ Bn	0.000224
22	source	1
23	I κ B α -t	0.005503
24	sink	0
25	I κ B β -t	0.000636
26	I κ B ϵ -t	0.000454

A.2 Healthy NF- κ B model reactions and their rates

Reaction Name	Reaction	Symbol	Rate
$I_{\kappa}B_{\alpha}NF_{-\kappa}B$ -association	$I_{\kappa}B_{\alpha} + NF_{-\kappa}B \rightarrow I_{\kappa}B_{\alpha}NF_{-\kappa}B$	k-1	0.5
$I_{\kappa}B_{\alpha}NF_{-\kappa}B$ -dissociation	$I_{\kappa}B_{\alpha}NF_{-\kappa}B \rightarrow NF_{-\kappa}B + I_{\kappa}B_{\alpha}$	k-2	0.0005
$I_{\kappa}B_{\beta}NF_{-\kappa}B$ -association	$I_{\kappa}B_{\beta} + NF_{-\kappa}B \rightarrow I_{\kappa}B_{\beta}NF_{-\kappa}B$	k-3	0.5
$I_{\kappa}B_{\beta}NF_{-\kappa}B$ -dissociation	$I_{\kappa}B_{\beta}NF_{-\kappa}B \rightarrow NF_{-\kappa}B + I_{\kappa}B_{\beta}$	k-4	0.0005
$I_{\kappa}B_{\epsilon}NF_{-\kappa}B$ -association	$I_{\kappa}B_{\epsilon} + NF_{-\kappa}B \rightarrow I_{\kappa}B_{\epsilon}NF_{-\kappa}B$	k-5	0.5
$I_{\kappa}B_{\epsilon}NF_{-\kappa}B$ -dissociation	$I_{\kappa}B_{\epsilon}NF_{-\kappa}B \rightarrow NF_{-\kappa}B + I_{\kappa}B_{\epsilon}$	k-6	0.0005
IKKI $I_{\kappa}B_{\alpha}NF_{-\kappa}B$ -association	$IKKI_{\kappa}B_{\alpha} + NF_{-\kappa}B \rightarrow IKKI_{\kappa}B_{\alpha}NF_{-\kappa}B$	k-7	0.5
IKKI $I_{\kappa}B_{\alpha}NF_{-\kappa}B$ -dissociation	$IKKI_{\kappa}B_{\alpha}NF_{-\kappa}B \rightarrow NF_{-\kappa}B + IKKI_{\kappa}B_{\alpha}$	k-8	0.0005
IKKI $I_{\kappa}B_{\alpha}NF_{-\kappa}B$ -catalysis	$IKKI_{\kappa}B_{\alpha}NF_{-\kappa}B \rightarrow IKK + NF_{-\kappa}B$	k-9	0.0204
IKKI $I_{\kappa}B_{\beta}NF_{-\kappa}B$ -association	$IKKI_{\kappa}B_{\beta} + NF_{-\kappa}B \rightarrow IKKI_{\kappa}B_{\beta}NF_{-\kappa}B$	k-10	0.5
IKKI $I_{\kappa}B_{\beta}NF_{-\kappa}B$ -dissociation	$IKKI_{\kappa}B_{\beta}NF_{-\kappa}B \rightarrow NF_{-\kappa}B + IKKI_{\kappa}B_{\beta}$	k-11	0.0005
IKKI $I_{\kappa}B_{\beta}NF_{-\kappa}B$ -catalysis	$IKKI_{\kappa}B_{\beta}NF_{-\kappa}B \rightarrow IKK + NF_{-\kappa}B$	k-12	0.0075
IKKI $I_{\kappa}B_{\epsilon}NF_{-\kappa}B$ -association	$IKKI_{\kappa}B_{\epsilon} + NF_{-\kappa}B \rightarrow IKKI_{\kappa}B_{\epsilon}NF_{-\kappa}B$	k-13	0.5
IKKI $I_{\kappa}B_{\epsilon}NF_{-\kappa}B$ -dissociation	$IKKI_{\kappa}B_{\epsilon}NF_{-\kappa}B \rightarrow NF_{-\kappa}B + IKKI_{\kappa}B_{\epsilon}$	k-14	0.0005
IKKI $I_{\kappa}B_{\epsilon}NF_{-\kappa}B$ -catalysis	$IKKI_{\kappa}B_{\epsilon}NF_{-\kappa}B \rightarrow IKK + NF_{-\kappa}B$	k-15	0.011
$I_{\kappa}B_{\alpha}$ -constitutive-degradation-complexed-to-NF- κ B	$I_{\kappa}B_{\alpha}NF_{-\kappa}B \rightarrow NF_{-\kappa}B$	k-16	2.25E-05

$I_{\kappa}B\beta$ -constitutive-degradation-complexed-to-NF- κ B	$I_{\kappa}B\beta$ -NF- κ B -> NF- κ B	k-17	2.25E-05
$I_{\kappa}B\epsilon$ -constitutive-degradation-complexed-to-NF- κ B	$I_{\kappa}B\epsilon$ -NF- κ B -> NF- κ B	k-18	2.25E-05
NF- κ B-nuclear-import	NF- κ B -> NF- κ Bn	k-19	0.09
NF- κ B-nuclear-export	NF- κ Bn -> NF- κ B	k-20	8.00E-05
$I_{\kappa}B\alpha$ -NF- κ B-nuclear-association	$I_{\kappa}B\alpha$ n + NF- κ Bn -> $I_{\kappa}B\alpha$ n-NF- κ Bn	k-21	0.5
$I_{\kappa}B\alpha$ -NF- κ B-nuclear-dissociation	$I_{\kappa}B\alpha$ n-NF- κ Bn -> NF- κ Bn + $I_{\kappa}B\alpha$ n	k-22	0.0005
$I_{\kappa}B\beta$ -NF- κ B-nuclear-association	$I_{\kappa}B\beta$ n + NF- κ Bn -> $I_{\kappa}B\beta$ n-NF- κ Bn	k-23	0.5
$I_{\kappa}B\beta$ -NF- κ B-nuclear-dissociation	$I_{\kappa}B\beta$ n-NF- κ Bn -> NF- κ Bn + $I_{\kappa}B\beta$ n	k-24	0.0005
$I_{\kappa}B\epsilon$ -NF- κ B-nuclear-association	$I_{\kappa}B\epsilon$ n + NF- κ Bn -> $I_{\kappa}B\epsilon$ n-NF- κ Bn	k-25	0.5
$I_{\kappa}B\epsilon$ -NF- κ B-nuclear-dissociation	$I_{\kappa}B\epsilon$ n-NF- κ Bn -> NF- κ Bn + $I_{\kappa}B\epsilon$ n	k-26	0.0005
constitutive- $I_{\kappa}B\alpha$ -mRNA-synthesis	source -> $I_{\kappa}B\alpha$ -t	k-27	1.54E-06
$I_{\kappa}B\alpha$ -Inducible-mRNA-synthesis	NF- κ Bn + NF- κ Bn -> $I_{\kappa}B\alpha$ t + NF- κ Bn + NF- κ Bn	k-28	0.0165
$I_{\kappa}B\alpha$ -mRNA-degradation	$I_{\kappa}B\alpha$ -t -> sink	k-29	0.00028
constitutive- $I_{\kappa}B\beta$ -mRNA-synthesis	source -> $I_{\kappa}B\beta$ -t	k-30	1.78E-07
$I_{\kappa}B\beta$ -mRNA-degradation	$I_{\kappa}B\beta$ -t -> sink	k-31	0.00028
constitutive- $I_{\kappa}B\epsilon$ -mRNA-synthesis	source -> $I_{\kappa}B\epsilon$ -t	k-32	1.27E-07
$I_{\kappa}B\epsilon$ -mRNA-degradation	$I_{\kappa}B\epsilon$ -t -> sink	k-33	0.00028
IKK $I_{\kappa}B\alpha$ -association	IKK + $I_{\kappa}B\alpha$ -> IKK $I_{\kappa}B\alpha$	k-34	0.0225
IKK $I_{\kappa}B\alpha$ -dissociation	IKK $I_{\kappa}B\alpha$ -> IKK + $I_{\kappa}B\alpha$	k-35	0.00125

$I_{\kappa}B_{\alpha}$ -translation-rate	$I_{\kappa}B_{\alpha-t} \rightarrow I_{\kappa}B_{\alpha} + I_{\kappa}B_{\alpha-t}$	k-36	0.00408
constitutive- $I_{\kappa}B_{\alpha}$ -degradation-free	$I_{\kappa}B_{\alpha} \rightarrow \text{sink}$	k-37	0.000113
$I_{\kappa}B_{\alpha}$ -nuclear-import	$I_{\kappa}B_{\alpha} \rightarrow I_{\kappa}B_{\alpha n}$ (Import)	k-38	0.0003
$I_{\kappa}B_{\alpha}$ -nuclear-export	$I_{\kappa}B_{\alpha n} \rightarrow I_{\kappa}B_{\alpha}$ (Export)	k-39	0.0002
$IKKI_{\kappa}B_{\beta}$ -association	$IKK + I_{\kappa}B_{\beta} \rightarrow IKKI_{\kappa}B_{\beta}$	k-40	0.006
$IKKI_{\kappa}B_{\beta}$ -dissociation	$IKKI_{\kappa}B_{\beta} \rightarrow IKK + I_{\kappa}B_{\beta}$	k-41	0.00175
$I_{\kappa}B_{\beta}$ -translation-rate	$I_{\kappa}B_{\beta-t} \rightarrow I_{\kappa}B_{\beta} + I_{\kappa}B_{\beta-t}$	k-42	0.00408
constitutive- $I_{\kappa}B_{\beta}$ -degradation-free	$I_{\kappa}B_{\beta} \rightarrow \text{sink}$	k-43	0.000113
$I_{\kappa}B_{\beta}$ -nuclear-import	$I_{\kappa}B_{\beta} \rightarrow I_{\kappa}B_{\beta n}$ (Import)	k-44	0.00015
$I_{\kappa}B_{\beta}$ -nuclear-export	$I_{\kappa}B_{\beta n} \rightarrow I_{\kappa}B_{\beta}$ (Export)	k-45	0.0001
$IKKI_{\kappa}B_{\epsilon}$ -association	$IKK + I_{\kappa}B_{\epsilon} \rightarrow IKKI_{\kappa}B_{\epsilon}$	k-46	0.009
$IKKI_{\kappa}B_{\epsilon}$ -dissociation	$IKKI_{\kappa}B_{\epsilon} \rightarrow IKK + I_{\kappa}B_{\epsilon}$	k-47	0.00175
$I_{\kappa}B_{\epsilon}$ -translation-rate	$I_{\kappa}B_{\epsilon-t} \rightarrow I_{\kappa}B_{\epsilon} + I_{\kappa}B_{\epsilon-t}$	k-48	0.00408
constitutive- $I_{\kappa}B_{\epsilon}$ -degradation-free	$I_{\kappa}B_{\epsilon} \rightarrow \text{sink}$	k-49	0.000113
$I_{\kappa}B_{\epsilon}$ -nuclear-import	$I_{\kappa}B_{\epsilon} \rightarrow I_{\kappa}B_{\epsilon n}$ (Import)	k-50	0.00015
$I_{\kappa}B_{\epsilon}$ -nuclear-export	$I_{\kappa}B_{\epsilon n} \rightarrow I_{\kappa}B_{\epsilon}$ (Export)	k-51	0.0001
$IKK-I_{\kappa}B_{\alpha}NF-_{\kappa}B$ -association	$IKK + I_{\kappa}B_{\alpha}NF-_{\kappa}B \rightarrow IKKI_{\kappa}B_{\alpha}NF-_{\kappa}B$	k-52	0.185
$IKK-I_{\kappa}B_{\alpha}NF-_{\kappa}B$ -dissociation	$IKKI_{\kappa}B_{\alpha}NF-_{\kappa}B \rightarrow IKK + I_{\kappa}B_{\alpha}NF-_{\kappa}B$	k-53	0.00125
$I_{\kappa}B_{\alpha}NF-_{\kappa}B$ -nuclear-export	$I_{\kappa}B_{\alpha n}NF-_{\kappa}Bn \rightarrow I_{\kappa}B_{\alpha}NF-_{\kappa}B$ (Export)	k-54	0.0138

IKK-I κ B β NF- κ B-association	KK + I κ B β NF- κ B -> IKKI κ B β NF- κ B	k-55	0.048
IKK-I κ B β NF- κ B-dissociation	IKKI κ B β NF- κ B -> IKK + I κ B β NF- κ B	k-56	0.00175
I κ B β -NF- κ B-nuclear-export	I κ B β n-NF- κ Bn -> I κ B β NF- κ B (Export)	k-57	0.0052
IKK-I κ B ϵ NF- κ B-association	IKK + I κ B ϵ NF- κ B -> IKKI κ B ϵ NF- κ B	k-58	0.07
IKK-I κ B ϵ NF- κ B-dissociation	IKKI κ B ϵ NF- κ B -> IKK + I κ B ϵ NF- κ B	k-59	0.00175
I κ B ϵ -NF- κ B-nuclear-export	I κ B ϵ n-NF- κ Bn -> I κ B ϵ NF- κ B (Export)	k-60	0.0052
slow-adaptation	IKK -> sink	k-61	0.00012
IKKI κ B α -catalysis	IKKI κ B α -> IKK	k-62	0.00407
IKKI κ B β -catalysis	IKKI κ B β -> IKK	k-63	0.0015
IKKI κ B ϵ -catalysis	IKKI κ B ϵ -> IKK	k-64	0.0022

Appendix B

Figures

B.1 NF- κ B Model

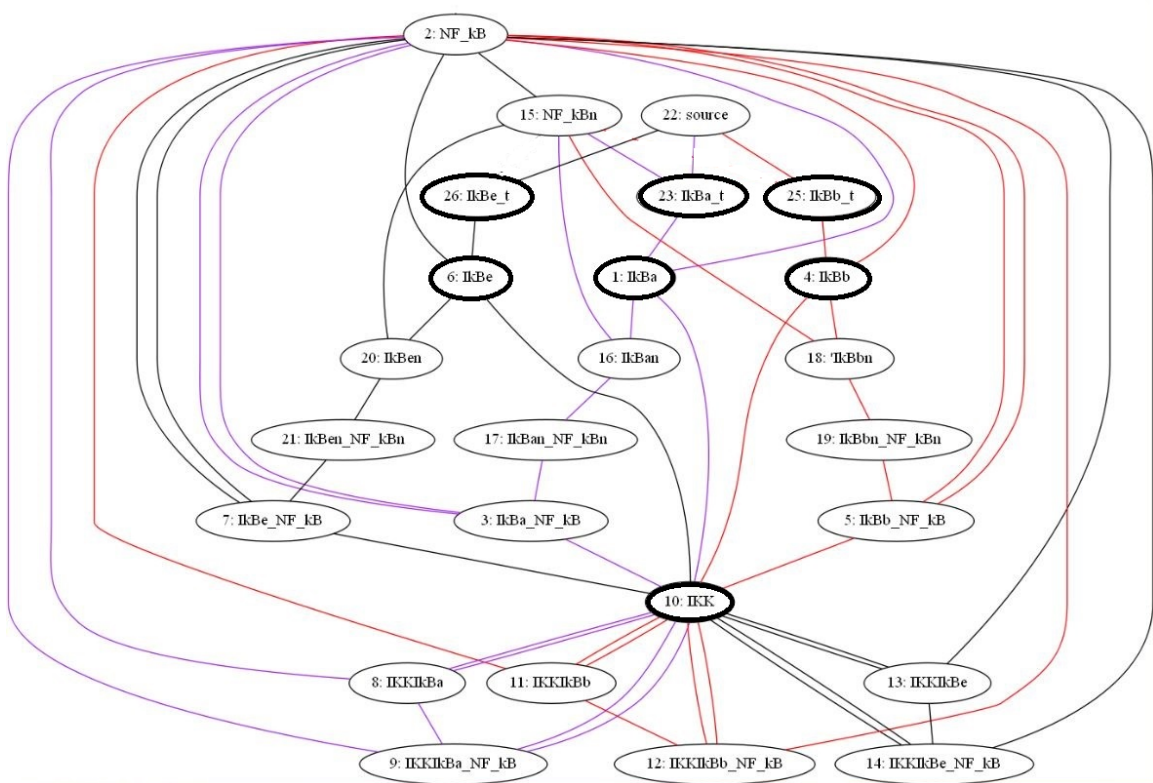
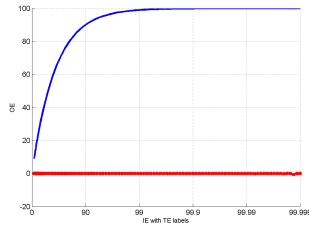
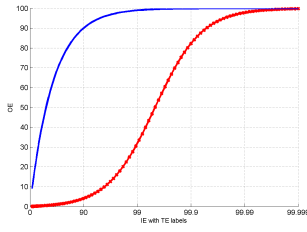


Figure B-1: NF- κ B model. Species encircled in darker boundaries get degraded

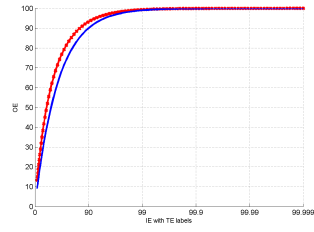
B.2 OE vs TE Species Profiles for the Healthy Model



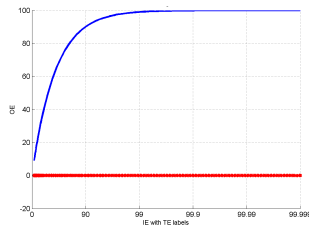
(a) 1: $I\kappa B\alpha$



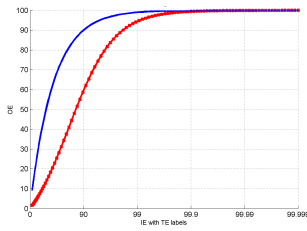
(b) 2: $NF-\kappa B$



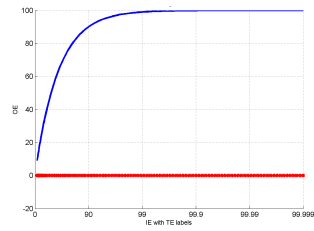
(c) 3: $I\kappa B\alpha-NF-\kappa B$



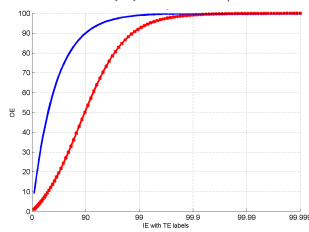
(d) 4: $I\kappa B\beta$



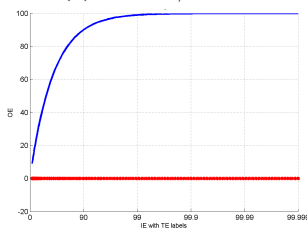
(e) 5: $I\kappa B\beta-NF-\kappa B$



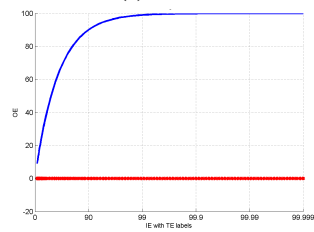
(f) 6: $I\kappa B\epsilon$



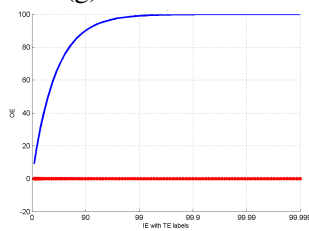
(g) 7: $I\kappa B\epsilon-NF-\kappa B$



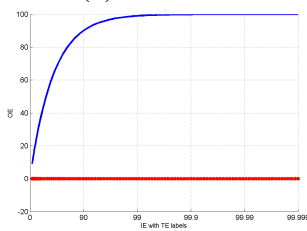
(h) 8: $IKK I\kappa B\alpha$



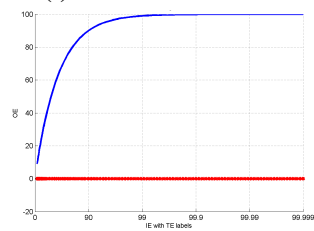
(i) 9: $IKK I\kappa B\alpha-NF-\kappa B$



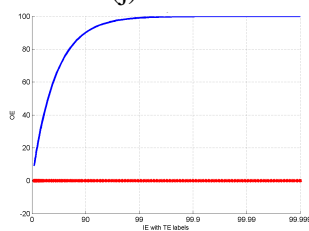
(j) 10: IKK



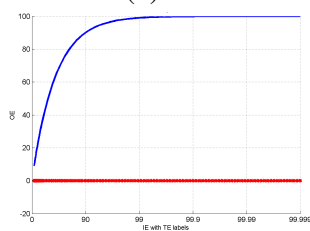
(k) 11: $IKK I\kappa B\beta$



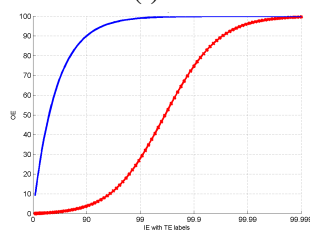
(l) 12: $IKK I\kappa B\beta-NF-\kappa B$



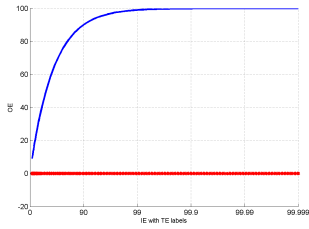
(m) 13: $IKK I\kappa B\epsilon$



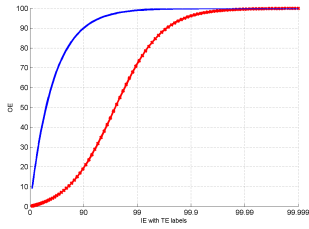
(n) 14: $IKK I\kappa B\epsilon-NF-\kappa B$



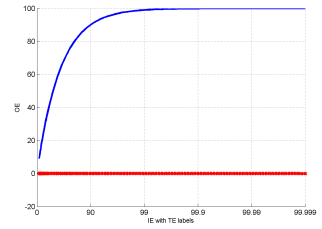
(o) 15: $NF-\kappa Bn$



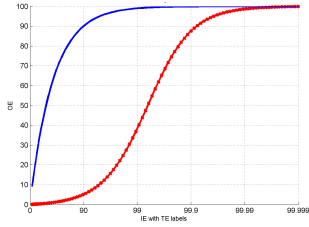
(p) 16: $I\kappa B\alpha n$



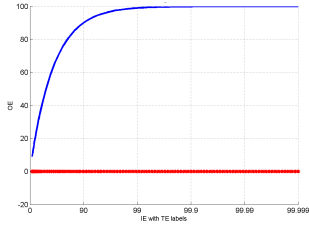
(q) 17: $I\kappa B\alpha n-NF-\kappa B n$



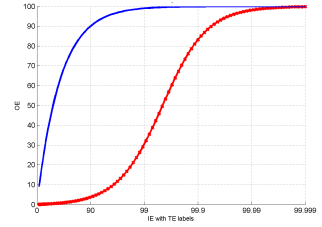
(r) 18: $I\kappa B\beta n$



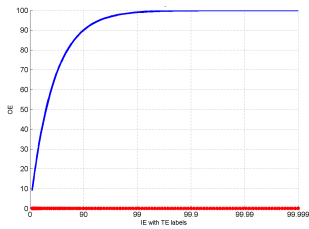
(s) 19: $I\kappa B\beta n-NF-\kappa B n$



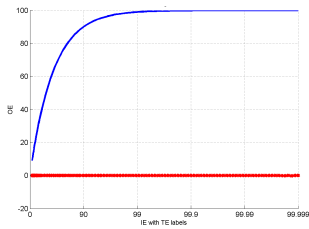
(t) 20: $I\kappa B\epsilon n$



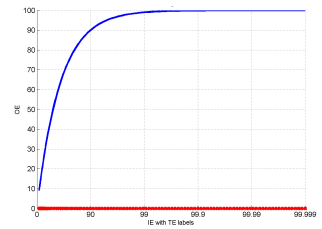
(u) 21: $I\kappa B\epsilon n-NF-\kappa B n$



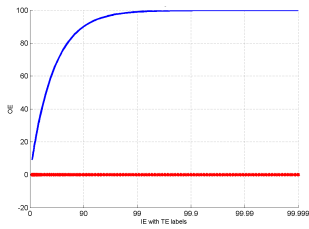
(v) 22: Source



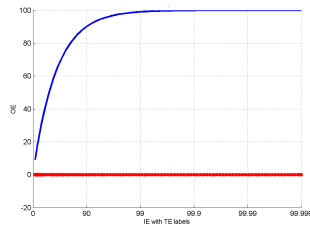
(w) 23: $I\kappa B\alpha-t$



(x) 24: Sink

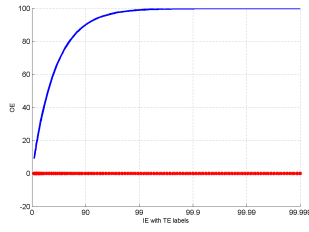


(y) 25: $I\kappa B\beta-t$

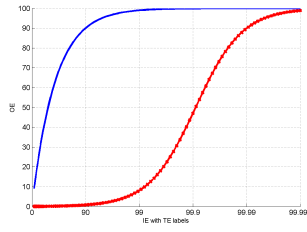


(z) 26: $I\kappa B\epsilon-t$

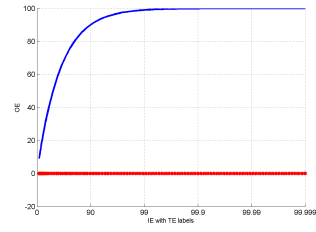
B.3 OE vs TE Species Profiles for Disease Model 1



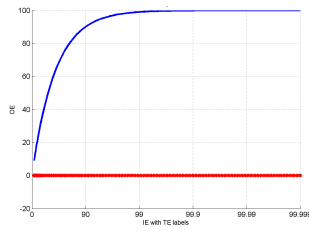
(a) 1: $I\kappa B\alpha$



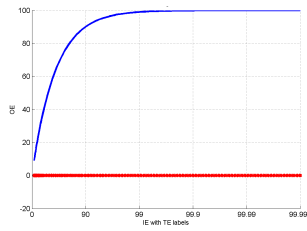
(b) 2: $NF-\kappa B$



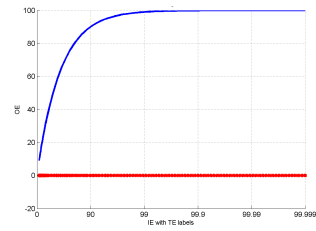
(c) 3: $I\kappa B\alpha-NF-\kappa B$



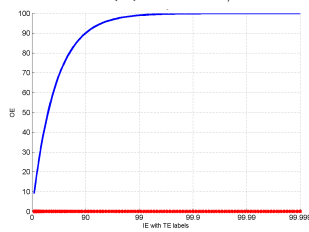
(d) 4: $I\kappa B\beta$



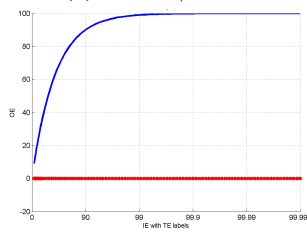
(e) 5: $I\kappa B\beta-NF-\kappa B$



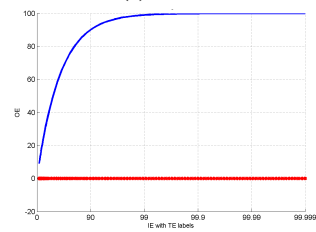
(f) 6: $I\kappa B\epsilon$



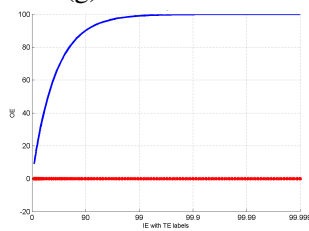
(g) 7: $I\kappa B\epsilon-NF-\kappa B$



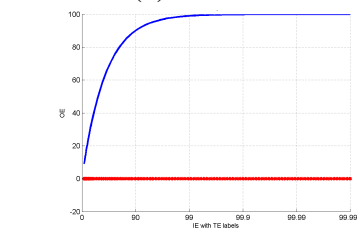
(h) 8: $IKKI\kappa B\alpha$



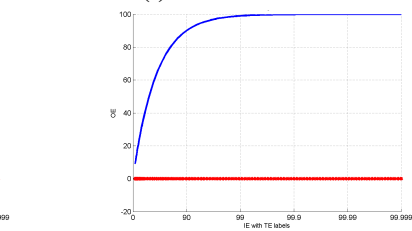
(i) 9: $IKKI\kappa B\alpha-NF-\kappa B$



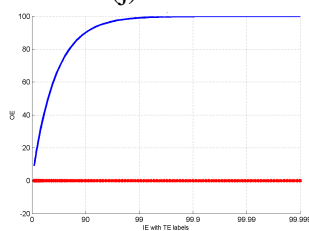
(j) 10: IKK



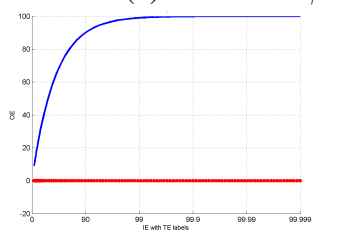
(k) 11: $IKKI\kappa B\beta$



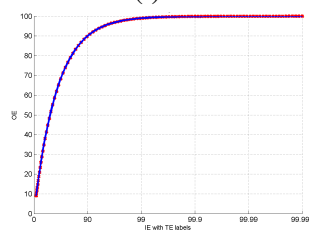
(l) 12: $IKKI\kappa B\beta-NF-\kappa B$



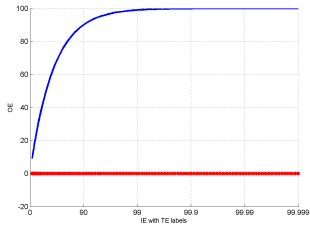
(m) 13: $IKKI\kappa B\epsilon$



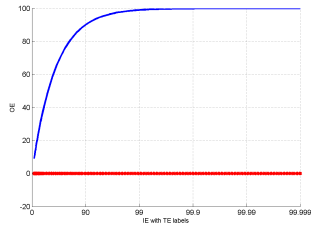
(n) 14: $IKKI\kappa B\epsilon-NF-\kappa B$



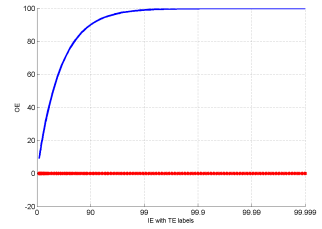
(o) 15: $NF-\kappa Bn$



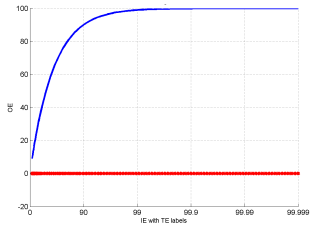
(p) 16: $I\kappa B\alpha n$



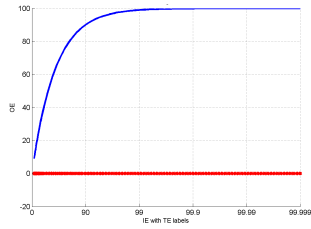
(q) 17: $I\kappa B\alpha n - NF-\kappa B n$



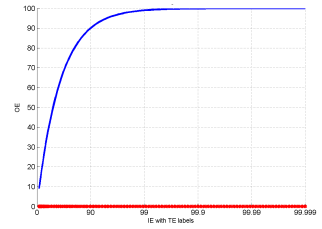
(r) 18: $I\kappa B\beta n$



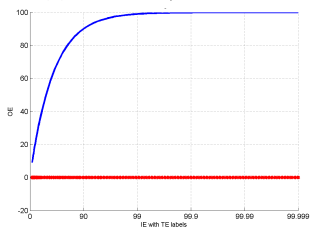
(s) 19: $I\kappa B\beta n - NF-\kappa B n$



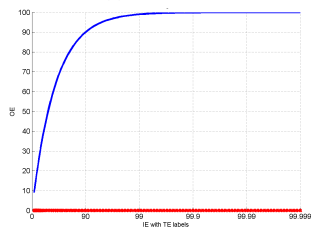
(t) 20: $I\kappa B\epsilon n$



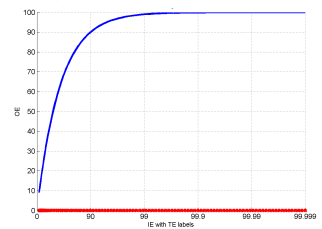
(u) 21: $I\kappa B\epsilon n - NF-\kappa B n$



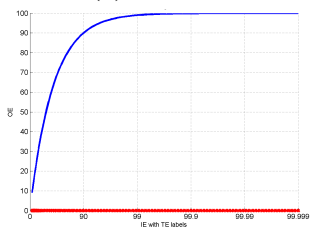
(v) 22: Source



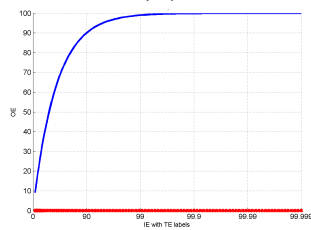
(w) 23: $I\kappa B\alpha - t$



(x) 24: Sink

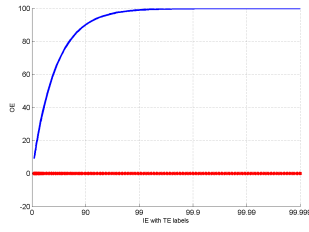


(y) 25: $I\kappa B\beta - t$

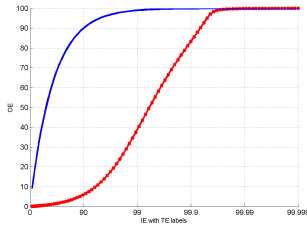


(z) 26: $I\kappa B\epsilon - t$

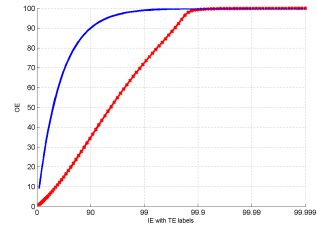
B.4 OE vs TE Species Profiles for Disease Model 3



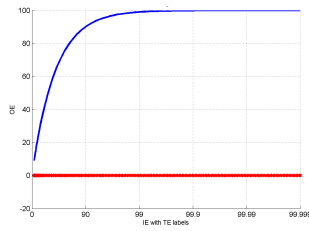
(a) 1: $I\kappa B\alpha$



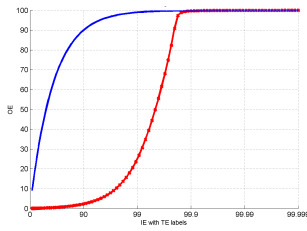
(b) 2: $NF-\kappa B$



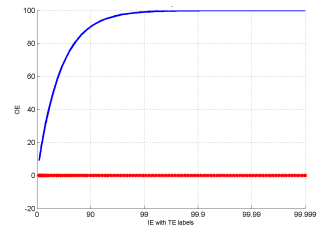
(c) 3: $I\kappa B\alpha-NF-\kappa B$



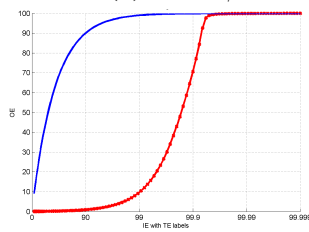
(d) 4: $I\kappa B\beta$



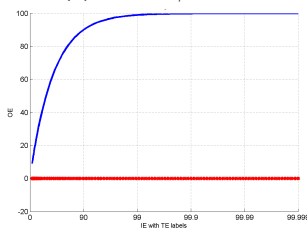
(e) 5: $I\kappa B\beta-NF-\kappa B$



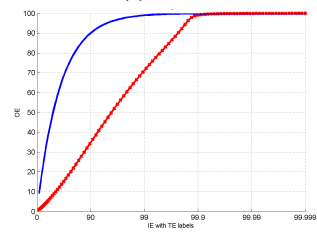
(f) 6: $I\kappa B\epsilon$



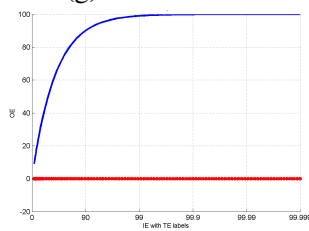
(g) 7: $I\kappa B\epsilon-NF-\kappa B$



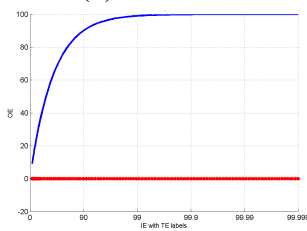
(h) 8: $IKK1\kappa B\alpha$



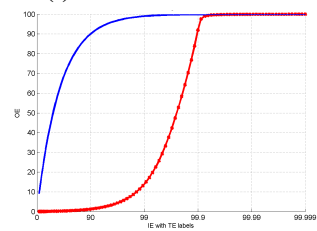
(i) 9: $IKK1\kappa B\alpha-NF-\kappa B$



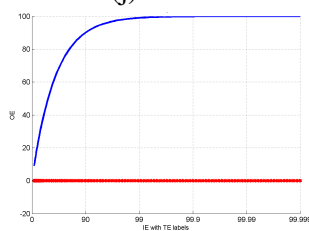
(j) 10: IKK



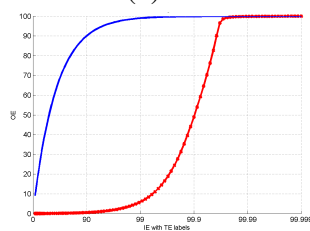
(k) 11: $IKK1\kappa B\beta$



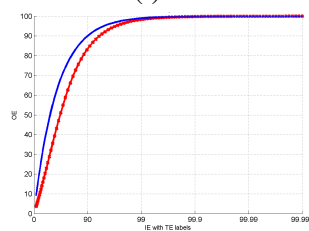
(l) 12: $IKK1\kappa B\beta-NF-\kappa B$



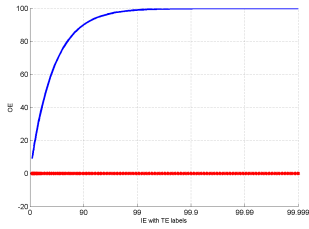
(m) 13: $IKK1\kappa B\epsilon$



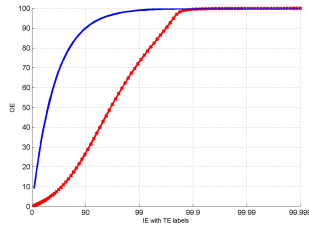
(n) 14: $IKK1\kappa B\epsilon-NF-\kappa B$



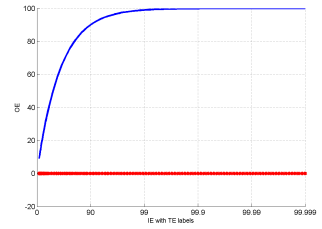
(o) 15: $NF-\kappa Bn$



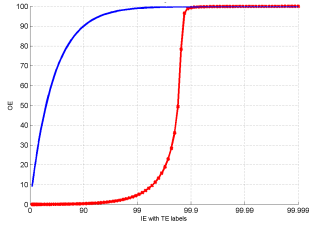
(p) 16: $I\kappa B\alpha n$



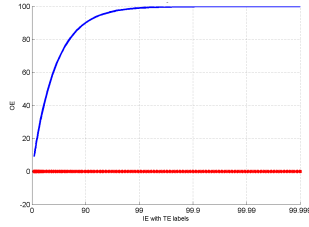
(q) 17: $I\kappa B\alpha n-NF-\kappa B n$



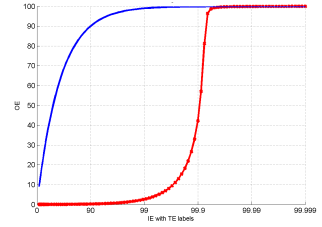
(r) 18: $I\kappa B\beta n$



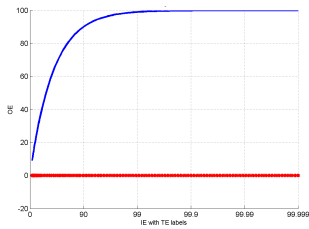
(s) 19: $I\kappa B\beta n-NF-\kappa B n$



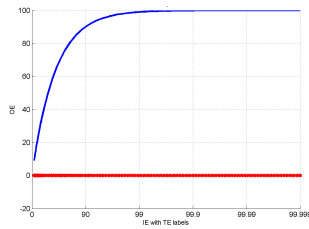
(t) 20: $I\kappa B\epsilon n$



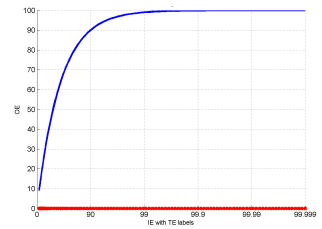
(u) 21: $I\kappa B\epsilon n-NF-\kappa B n$



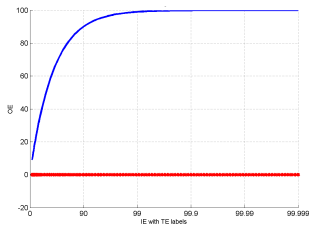
(v) 22: Source



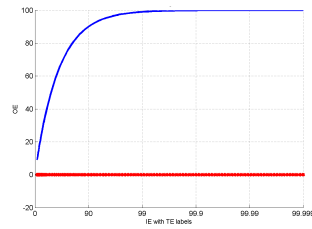
(w) 23: $I\kappa B\alpha-t$



(x) 24: Sink



(y) 25: $I\kappa B\beta-t$



(z) 26: $I\kappa B\epsilon-t$

B.5 Synergism Classifications

Plots of synergism classification of each combination of pairs at various OE levels for various model. Circle size varies according to OE levels and circle colors correspond to different classes. Red circles are synergistic, green circles are additive, and blue circles are antagonistic. The pairs that do not have any associated circles do not achieve any of the following seven OE levels: 30 %, 50 %, 70 %, 90 %, 99.0 %, 99.99 %, and 99.999 %.

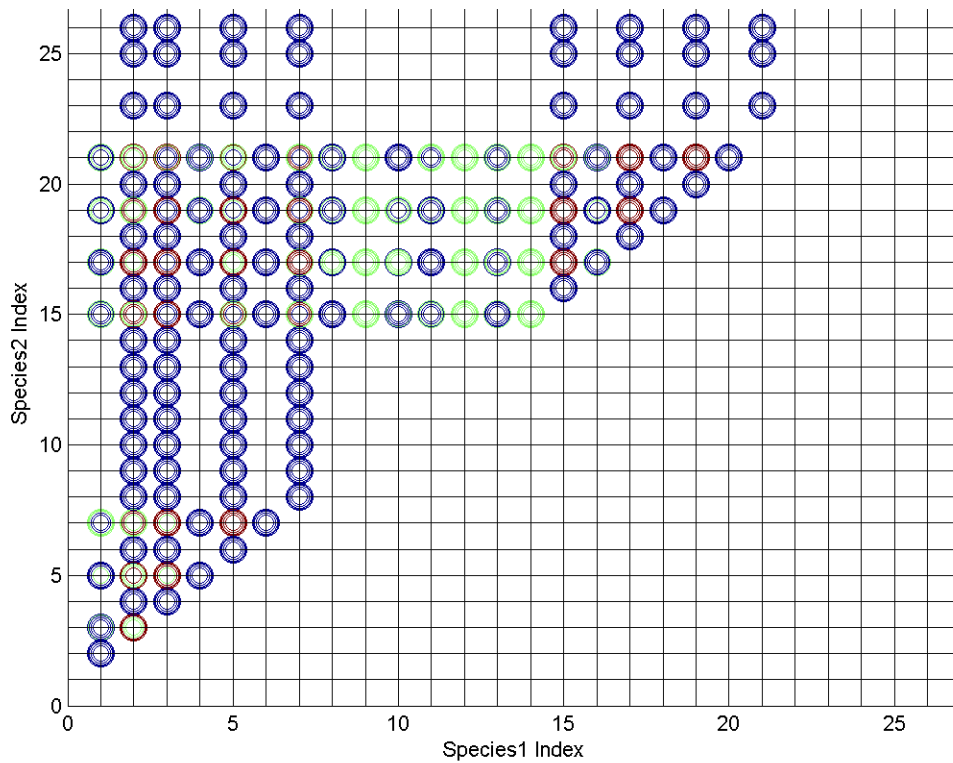


Figure B-5: Synergism classification for all combinations of species in the healthy model.

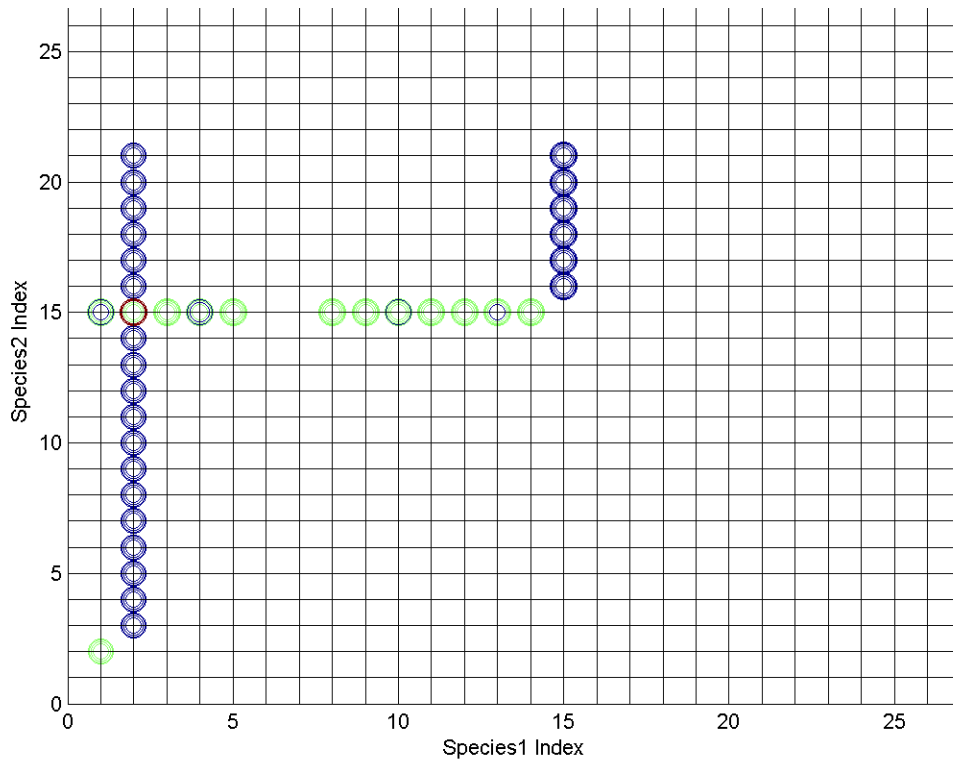


Figure B-6: Synergism classification for all combinations of species in disease model 1.

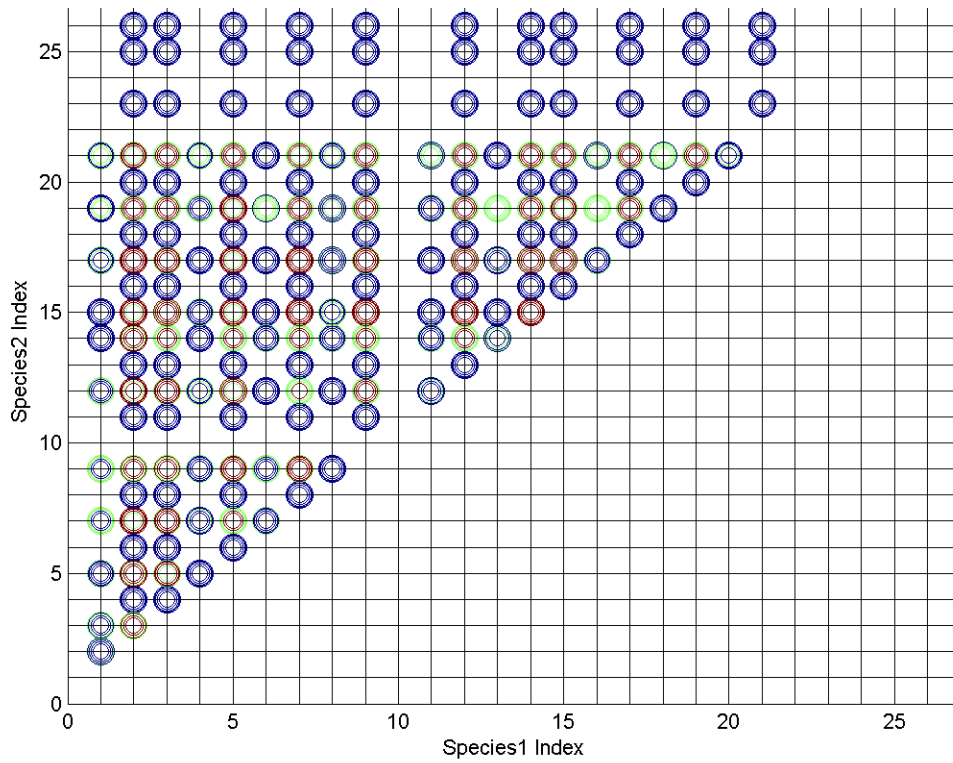


Figure B-7: Synergism classification for all combinations of species in disease model 3.

Bibliography

- [1] Oeckinghaus, Andrea, and Sankar Ghosh. "The NF- κ B family of transcription factors and its regulation." *Cold Spring Harbor perspectives in biology* 1.4 (2009): a000034.
- [2] Baker, Rebecca G., Matthew S. Hayden, and Sankar Ghosh. "NF- κ B, inflammation, and metabolic disease." *Cell metabolism* 13.1 (2011): 11-22.
- [3] Tak, Paul P., and Gary S. Firestein. "NF- κ B: a key role in inflammatory diseases." *The Journal of clinical investigation* 107.1 (2001): 7-11.
- [4] Luron, Lionel, et al. "FOXO3 as a new IKK ϵ controlled checkpoint of regulation of IFN β expression." *European journal of immunology* 42.4 (2012): 1030-1037.
- [5] Trepicchio, William L., and Andrew J. Dorner. "Interleukin11: A gp130 Cytokine." *Annals of the New York Academy of Sciences* 856.1 (1998): 12-21.
- [6] Gohda, Jin, Jun-Ichiro Inoue, and Kazuo Umezawa. "Down-regulation of TNF- α receptors by conophylline in human T-cell leukemia cells." *International journal of oncology* 23.5 (2003): 1373-1379.
- [7] Miller, Susanne C., et al. "Identification of known drugs that act as inhibitors of NF- κ B signaling and their mechanism of action." *Biochemical pharmacology* 79.9 (2010): 1272-1280.
- [8] Peng, Huiming, et al. "Drug inhibition profile prediction for NF κ B pathway in multiple myeloma." *PloS one* 6.3 (2011): e14750.
- [9] Ihekweba, A. E. C., et al. "Sensitivity analysis of parameters controlling oscillatory signalling in the NF- κ B pathway: the roles of IKK and I κ B α ." *Syst Biol* 1 (2004): 93-103.
- [10] Tilstra, Jeremy S., et al. "NF- κ B in aging and disease." *Aging and disease* 2.6 (2014): 449-465.
- [11] NF- κ B signaling, *Cell signaling technology* (2012)
- [12] Courtois, G., and T. D. Gilmore. "Mutations in the NF- κ B signaling pathway: implications for human disease." *Oncogene* 25.51 (2006): 6831-6843.
- [13] Schmidt-Supprian, Marc, et al. "NEMO/IKK β -deficient mice model incontinentia pigmenti." *Molecular cell* 5.6 (2000): 981-992.

- [14] Keats, Jonathan J., et al. "Promiscuous mutations activate the noncanonical NF- κ B pathway in multiple myeloma." *Cancer cell* 12.2 (2007): 131-144.
- [15] Paudel, Nirmala. Computational analysis of biochemical networks for drug target identification and therapeutic intervention design. Diss. Massachusetts Institute of Technology, 2014.
- [16] Hornbeck, Peter V., et al. "PhosphoSitePlus: a comprehensive resource for investigating the structure and function of experimentally determined post-translational modifications in man and mouse." *Nucleic acids research* (2011): gkr1122.
- [17] Xiong, Huabao, et al. "Interaction of TRAF6 with MAST205 regulates NF- κ B activation and MAST205 stability." *Journal of Biological Chemistry* 279.42 (2004): 43675-43683.
- [18] Martin, Gregoire, et al. "Rhein inhibits interleukin-1 β -induced activation of MEK/ERK pathway and DNA binding of NF- κ B and AP-1 in chondrocytes cultured in hypoxia: a potential mechanism for its disease-modifying effect in osteoarthritis." *Inflammation* 27.4 (2003): 233-246.
- [19] Shukla, Sanjeev, and Sanjay Gupta. "Suppression of constitutive and tumor necrosis factor α -induced nuclear factor (NF)- κ B activation and induction of apoptosis by apigenin in human prostate carcinoma PC-3 cells: correlation with down-regulation of NF- κ B-responsive genes." *Clinical Cancer Research* 10.9 (2004): 3169-3178.
- [20] TaiPing, H. E., M. O. LiEr, and L. I. A. N. G. NianCi. "Inhibitory Effect of Cantharidin on Invasion and Metastasis of Highly Metastatic Ovarian Carcinoma Cell Line HO 8910PM." *chinese Journal of cancer* 24.4 (2005): 443V447.